Familial ALS Proteins Function in Prevention/repair of Transcription-Associated DNA Damage

Abstract:

Amyotrophic lateral sclerosis (ALS) is a progressive motor neuron dysfunction disease that leads to paralysis and death. There is currently no defined molecular pathogenesis pathway. Multiple proteins involved in RNA processing are linked to ALS, including FUS and TDP43; and we propose a disease mechanism in which loss of function of one of these proteins leads to an accumulation of transcription-associated DNA damage contributing to motor neuron cell death and progressive neurological symptoms.

In support of this hypothesis, we found that depletion of FUS and TDP43 leads to increased sensitivity to a transcription-arresting agent due to increased DNA damage. This indicates that these proteins normally contribute to the prevention or repair of transcription-associated DNA damage. In addition, we observed that both FUS and TDP43 co-localize with active RNA polymerase II at sites of DNA damage along with the DNA damage repair protein BRCA1, and that FUS and TDP43 participate in the prevention or repair of R-loop associated DNA damage.

Ideally, gaining a better understanding of the role(s) that FUS and TDP43 play in transcription-associated DNA damage will shed light on the mechanisms underlying ALS pathogenesis.

Table of Contents **Page Number**

Glossary of Abbreviations:

ALS-Amyotrohpic Lateral Sclerosis

BER-Base Excision Repair

DAPI-4',6-diamidino-2-phenylindole

DSB-Double Strand Break

fALS-Familial Amyotrohpic Lateral Sclerosis

FET-FUS, EWSR1, TAF15

FTLD-Fronto-Temporal Lobar Dementia

HR-Homologous Recombination

iPSC-induced pluripotent stem cell

LC-Low complexity

NER-Nucleotide Excision Repair

NHEJ-Non-homologous end joining

RNAPolII-RNA Polymerase II

siRNA-short interfering RNA

UV-Ultraviolet

Introduction:

Amyotrophic lateral sclerosis (ALS) is a disease of both upper and lower motor neuron dysfunction that leads to progressive paralysis and, eventually, death due to respiratory failure. No single model of disease pathogenesis for the motor neuron death in ALS has been revealed; however, many genes have been associated with the disease through genetic studies (1). The variability of function in these familial genes suggests that there may be multiple subtypes of ALS. Moreover, the familial ALS gene list is also enriched in protein groups with related functions.

Mutations in multiple RNA processing genes, including *FUS, TDP43, SETX*, *C9ORF72, TAF15, EWSR1, HNRNPA1,* and *HNRNPA2B1,* among others, are known to give rise to familial ALS [fALS] (1). However, FUS and TDP43 are currently the best studied, given that mutations in these genes lead to classic histologic findings in neural tissue from patients who die from ALS and that similar histologic findings can be found in neural tissue from typical sporadic cases of ALS. Specifically, cytoplasmic inclusions that contain ubiquitinated and phosphorylated proteins were recently identified in neural tissue from ALS patients at autopsy. After significant analysis, the proteins in these inclusions were identified as TDP43 (2). In certain families with mutations in FUS, they also included FUS (3). Analysis of familial and sporadic ALS autopsy neural tissue revealed the presence of TDP43 inclusions in the cytoplasm of motor neurons in ALS patients with a) TDP43 mutations and b) sporadic ALS (i.e. patients with no FUS, TDP43, SOD, or other pathogenic mutation) (4). They were also present in neurons in various parts of the brain in patients with either sporadic or familial versions of the ALS-related disorder, fronto-temporal lobar dementia (FTLD) (4). At autopsy, FUS inclusions were found in the cytoplasm of motor neurons in fALS patients with known FUS mutations and in the cytoplasm of neurons in different regions of the brain in some FTLD patients (4).

FUS and TDP43 exhibit a wide range of functions, mostly involving transcription and RNA processing. However, it is unclear what the discovery of these cytoplasmic inclusions in patients with sporadic and fALS mean with respect to disease pathogenesis and protein function. Conceivably, nuclear TDP43 and/or FUS undergo a toxic loss of function when the molecular pathways in which these proteins participate are disrupted. However, it is also possible that these cytoplasmic inclusions represent a toxic gain of function, i.e. the inclusions in the

cytoplasm are themselves toxic to the motor neurons over time, leading to motor neuron cell death and the ALS phenotype.

Recent protein phase analysis has shed some light on the formation of these aggregates. Both FUS and TDP43, along with many RNA binding proteins contain repetitive and possibly disordered functional domains referred to as low complexity (LC) or prion-like domains, and proteins containing these domains have been frequently shown to form membrane-less functional compartments within a cell (5, 6). Recent work indicates that FUS can assemble into such membrane-less compartments through its LC domain and that alterations in protein abundance or protein structure (i.e. due to an ALS linked mutation) may cause aberrant stabilization of these compartments (7-9).

FUS assembles into liquid or hydrogel compartments that are reversible in the WT state and moves between the nucleus and cytoplasm during different types of stress, including DNA damage, to form these compartments and carry out various molecular functions (7-9). fALS-linked mutant FUS also forms the liquid and hydrogel states but becomes stabilized in the hydrogel/fibrous state theoretically, leading to a decreased concentration of functional FUS or a toxic protein aggregate (7-9). The same stable aggregates can be derived in the setting of increased FUS concentration under specific conditions (8, 9). In C. elegans models, these stabilized protein aggregates lead to increased neurotoxicity which could be due to either loss of FUS function due to aggregation of functional protein or gain of toxic function of the stabilized hydrogels (8).

The stabilized FUS hydrogels contain other RNA binding proteins and components of RNP granules in the cytoplasm that could lead to decreased protein translation, which would be especially toxic for neurons with long axons, such as motor neurons (8). This setting might represent one associated with a possible toxic loss of FUS function and mechanism contributing to ALS pathogenesis (8). However, FUS has many other functions, including a role in DNA damage repair in which it forms a liquid compartment around DNA breaks and potentially recruits DNA damage repair proteins (9). This function could also be lost through stable hydrogel formation by mutant FUS in the cytoplasm, thereby again leading to motor neuron cell death and ALS (9). The importance of the cytoplasmic FUS aggregates or hydrogels, with respect to loss or gain of function, has not yet been fully appreciated and will require further analysis. Of equal importance is gaining a better understanding of the molecular functions of

ALS-linked proteins as part of an effort to determine which of these functions might be ALS-suppressing.

Multiple FUS and TDP43 mouse models have been generated, but none has yet perfectly recapitulated the classic histologic findings and/or the motor neuron dysfunction driven phenotypes typical of ALS (10). Despite this fact, animal models and cell-based assays have illuminated certain functions of FUS and TDP43 in both cycling and terminally differentiated cells (10-12). Work on TDP43 has suggested roles for it in transcription regulation, mRNA splicing and transport, and stress granule formation among other functions (11). FUS also plays a role in multiple cellular processes including transcription regulation, mRNA splicing and transport, stress granule formation, homologous DNA pairing through its DNA binding domain, and various forms of DNA damage repair (12). The evidence suggesting a role for FUS in DNA damage repair is particularly intriguing for ALS pathogenesis, given growing evidence that RNA binding proteins play a key role in the prevention of transcription-associated DNA damage and also in its repair (13-16). Other ALS related proteins including SETX, EWSR1, and TAF15, all RNA-binding proteins, have also been linked to DNA damage and repair, further suggesting the importance of this pathway in ALS. The importance of transcription-associated DNA damage has only recently been more thoroughly explored.

In a recent effort searching for proteins involved in DNA damage prevention, depletion of multiple RNA binding/processing proteins led to increased abundance of γH2AX foci, a canonical marker of DNA damage (15). This suggests that these proteins are important in either preventing or repairing DNA damage associated with transcription and RNA processing (15). In support of this notion, another study searching for proteins that localize to UV laser induced sites of DNA damage revealed that many transcription-related proteins, including the ALS linked TAF15 and EWSR1 proteins (1), localize to these sites of DNA damage, many in a PARP-dependent fashion (16). Upon further analysis, this work also revealed that 70% of randomly selected transcription factors localize to sites of UV laser-induced DNA damage further suggesting that transcription-related proteins play in important role in the prevention or repair of DNA damage (16).

DNA damage can arise from malfunction in multiple facets of transcription and RNA processing, in which some of the above ALS proteins are known to or likely participate. These include: a) collapse of transcription machinery at sites of DNA damage or other barriers and the

subsequent evolution of double strand DNA breaks [DSB]; b) collisions between transcription and replication machinery, again leading to DSBs; c) damage to genomic segments that have been opened up/prepared for transcription; and d) the formation and unnatural stabilization of DNA-RNA hybrid structures called R loops (these consist of a segment of the transcribed DNA strand bound to its nascent RNA transcript with the non-transcribed DNA strand looped out) which triggers the development of DNA damage (13, 15, 17, 18). Multiple ALS proteins have roles in the above noted functions.

SETX, a DNA/RNA helicase and fALS protein associated with a juvenile form of ALS, functions in the resolution of R loops. Accompanying SETX depletion or malfunction, there is an increase in DNA damage most likely caused by prolonged stabilization of R loops (19-21). Thus, loss of this function is a possible contributor to ALS pathogenesis in SETX mutation carriers. In one mutant SETX mouse model, no evidence of increased R loop formation and stabilization could be detected in SETX mutant mouse neural tissue (22). However, this mouse model did not recapitulate any of the neurologic phenotypes of ALS or other neurodegenerative disorders. Thus, it is possible that the lack of detectable R-loops and DNA damage in neural tissue is a product of the model not affecting neural tissue in the same way a known human SETX mutation might.

FUS, TAF15, and EWSR1, all linked to both sarcoma and ALS, all participate in DNA damage-related pathways (1, 23). The three proteins are part of the FET (FUS, EWSR1, TAF15) protein family, and all contain an LC domain, both DNA and RNA binding domains, and a ZnF domain (23). All three have been shown to rapidly localize to sites of DNA damage (16, 24-26) and to be PARylated after various forms of genotoxic stress (27), and both TAF15 and FUS require PARP for DNA damage localization (16, 24, 26). Little is known about the mechanism of action of TAF15 and EWSR1 at sites of DNA damage. However, EWSR1 is required for survival of both UV and IR induced DNA damage, and UV damage suppresses EWSR1 mediated alternative splicing (28, 29). More is known about the function of FUS in the DNA damage response.

FUS is important for both HR and non-homologous end joining (NHEJ)-directed repair of DSBs in human cell lines (12, 24, 25). This result has also been observed in mouse cortical neurons, in which FUS depletion resulted in decreased NHEJ repair of DSBs and increased DNA damage (25). FUS arrives at DSB sites prior to other DNA damage repair proteins such as NBS1

and γH2AX through a mechanism requiring PARP1 generated PAR moieties for recruitment (24-26). Once there, FUS forms a liquid phase compartment around the break recruiting other RNA binding and DNA damage repair proteins (9), and FUS depletion leads to decreased recruitment of DNA damage proteins like γH2AX and phosphorylated ATM to these sites (25). The C-terminus of FUS is important in pairing homologous DNA regions to form a D-loop, critical in HR mediated DSB repair (30-33). FUS is also necessary to recruit HDAC1 to sites of DNA damage (25), and although its mechanism of action at DNA damage sites is not well understood, HDAC1 has recently been implicated in the repair of DSBs (25, 34).

Studies of ALS-linked mutant forms of FUS have led to mixed results with respect to HR and NHEJ proficiency. However, one study revealed increased γH2AX foci in the nuclei of motor neurons from ALS patients with known FUS mutations, suggesting the possibility that DNA damage had contributed to motor neuron cell death in these patients (12, 25). However, γH2AX can also stain apoptotic cells, and apoptosis is a known pathway for cell death in ALS (35). Thus γH2AX staining might, at least in part, be depicting apoptotic cells with their intrinsic chromatin breaks. Studies with additional DNA damage markers could help to evaluate the possibility that DNA damage played a role in motor neuron cell death in FUS and TDP43 mutant brains. Moreover, if DNA damage plays a role in ALS pathogenesis, the nature and origin(s) of the DNA damage would need to be determined.

Motor neurons are terminally differentiated and in the G0 phase of the cell cycle, thus repair of DSBs cannot occur via error free HR and is thought to occur via the more error prone NHEJ (36). Single strand breaks, bulky adducts and or crosslinks, or oxidative stress are repaired through PARP mediated single strand break repair, nucleotide excision repair, or base excision repair respectively (36). Buildup of DNA damage in terminally differentiated motor neurons can eventually lead to motor neuron cell death and potentially ALS, thus any mechanism that leads to increased DNA damage could play a potential role in the pathogenesis of ALS.

Since loss of function of certain RNA binding proteins leads to transcription-associated DNA damage, and since several fALS proteins are RNA binding proteins that are active in the prevention and/or repair of DNA damage, the potential for such damage to play a role in the pathogenesis of ALS remains possible.

Thus, the focus of our work was to better understand the role of FUS and TDP43 in the prevention and/or repair of DNA damage, in particular that associated with transcription. A

better understanding of the type of DNA damage associated with FUS and TDP43 loss of function and/or the role these proteins play in preventing or repairing transcription-associated DNA damage can result in new insights into the pathogenesis of a subset of ALS.

**Please note that this thesis was adapted from my submitted manuscript from September 2015 which is currently under revision for resubmission (37).

Materials and Methods

Cell Culture: U2OS cells were grown in DMEM 10%FBS/1% penicillin/streptomycin at 37°C and 10% CO2.

siRNA sequences: siGL2 (Dharmacon Cat. # D-001100-01). siFUS #7 (Dharmacon Cat. # J-009497-07), GAUCAAUCCUCCAUGAGUA. siFUS #8 (Dharmacon Cat. # J-009497-08) GGACAGCAGAGUUACAGUG. siTDP43 #2 (Dharmacon Cat. #D-012394-02), GCUCAAGCAUGGAUUCUAA. siTDP43 #3 (Dharmacon Cat. #D-012394-03), CAAUAGCAAUAGACAGUUA.

siRNA Transfection: Cells were plated for transfection on day 1, transfected with 50 pmol each of various siRNAs using Lipofectamine RNAiMax Transfection Reagent (Life Technologies Cat. # 13778150) on days two and three, and assayed on day 4.

α-Amanitin sensitivity assay: α-Amanitin (Sigma Cat. #A2263) was dissolved in filtered ddH2O. Cells were plated on day one, transfected on days 2 and 3 as described above, and plated at appropriate densities for colony formation on day 4. Enough cells to form between 100 and 300 colonies were plated in triplicate for each transfection at each dose. The cells were allowed to settle for 4 hours at 37°C, and the media was changed to media containing various doses of α-Amanitin including 0uM (equivalent volume of water to that employed at the highest dose of α-Amanitin was added to this media), 0.025uM, 0.05uM, 0.075uM, 0.1uM, 0.125uM, 0.15uM, 0.175uM, 0.2uM, 0.225uM, 0.25uM, and 0.35uM. Cells were incubated in media containing α-Amanitin for 24 hours at 37°C. This media was then removed, the cells were washed once with PBS, fresh media containing no α-Amanitin was added, and the cells were allowed to incubate at 37°C until appropriate sized colonies had formed. Cells were then washed with PBS, stained with crystal violet solution, and dried. Colonies were counted using a Microbiology International ProtoCOL colony counter.

Statistical analysis was performed using GraphPad Prism software. The percentage of surviving cells compared to the 0uM α-Amanitin control for each dose and each siRNA was

calculated for each individual replicate in each experiment. These values were entered into GraphPad Prism to generate a dose curve to which a non-linear regression curve was fit for each individual siRNA in each experiment. The α-Amanitin IC50 was estimated for each siRNA in each experiment from this curve. The IC50s calculated from all replicates for each siRNA were averaged, and the values are shown in the bar graphs in Figure 1, with the error bars representing the standard deviation between the replicates. The p-values represent the significance of the differences between the IC50s for the control siRNA and the individual gene-specific siRNAs, and these were calculated using a paired, two-tailed t-test in GraphPad Prism. Dose curves representing the average value at each dose for all three replicates were also generated in GraphPad Prism. They are shown in Figure 1.

Comet assays: Cells were plated on day 1 and transfected with control or gene-specific siRNAs on days 2 and 3. On day 4, the medium was changed to medium containing 0.35uM α-Amanitin or an equivalent volume of water, and the cells were incubated in it for 24 hours at 37°C. On day 5, alkaline comet assays were performed on these cells using a Trevigen CometAssay Kit (VWR Cat. # 95036-942) according to the manufacturer's protocol. Photos of the comet tails were taken, and comet tail length was assessed using TriTek CometScore software. Four replicates of the experiment were performed for each siRNA. Statistical comparison of the significance of the differences between water and α-Amanitin treated cells was performed using GraphPad Prism software with a paired two-tailed T-test.

Motor Neuron Differentiation

Wildtype motor neurons were derived based on a previously described protocol (38) modified to use adherent cells, without producing embryoid body precursors, throughout the differentiation to motor neurons. Motor neurons were plated on chamber slides for UV treatment and immunofluorescence, as described below. After being plated on chamber slides, neurons were allowed to mature for at least two weeks prior to UV treatment and staining.

UV Immunofluorescence: All immunofluorescent staining was viewed and later photographed using a Zeiss Axioskop 2 MOT microscope.

For all experiments, cells were plated on coverslips on day 1. The fixation and staining method are briefly reviewed here (39, 40). After various treatments or transfections, cells were washed with PBS, fixed in chilled Methanol:Acetic Acid (3:1) at 4°C for 15 minutes, and then washed with PBS. Cells were exposed to Blocking Solution (1mg/mL BSA, 5% normal goat

serum, 1% Triton X-100, and PBS) at 37°C for 30 minutes and then washed in PBS. They were then incubated in primary and then secondary antibodies diluted in Blocking Solution. Finally, cells were mounted with mounting medium containing DAPI (Vector Laboratories Cat. # H-1200), and then viewed and photographed.

Primary and secondary antibodies included the following: Mouse anti-BRCA1 clone SD123 (41), Mouse anti-TDP43 (Abcam ab57105), Mouse anti-FUS (Santa Cruz sc-47711), Rabbit anti-FUS (Bethyl A300-302A), RNA polymerase II CTD repeat YSPTSPS (phospho S5) antibody (Abcam ab5131), Phospho RPA32 (S4/S8) (Bethyl Cat. #A300-245A), Rabbit anti-γH2AX antibody (Abcam #ab2893), Goat Anti-Rabbit IgG H&L (Alexa Fluor® 488) (Abcam ab150077), Goat Anti-Mouse IgG H&L (Alexa Fluor® 594) (Abcam ab150116).

For UV exposure, cells were plated on coverslips on day 1. On day 2, they were washed once with PBS, treated with either 25J or exposed to air for an equivalent amount of time (0J control), allowed to recover at 37°C for 4 hours, and then fixed and stained with the appropriate antibodies as described above. UV treatment was performed using a 254 nm UV-C lamp (UVP Inc., Upland, CA), and dosage was measured using a UVX radiometer (UVP Inc., Upland, CA). The UV exposure experiments were repeated three, separate times for each antibody pairing. Nuclei with greater than or equal to 3 co-localizing foci were counted in the 0J and 4 hours post 25J experiments, and the percentage of nuclei containing greater than or equal to 3 co-localizing foci compared to the total number of nuclei counted for the various antibody pairings was calculated for each experiment. The average percentage was calculated for the three, separate experiments for each antibody pairing, and is shown in the bar graphs in Figures 4, 5, 7, and 8 with the error bars representing the standard deviation between the three experiments. The p-values representing the significance of the difference between the 0J and 4 hour post 25J percentages were calculated using a paired, two-tailed T-test in Microsoft Excel.

For siRNA-treated cells, untreated cells were plated on coverslips on day 1, transfected with various siRNAs on days 2 and 3 as described above, and then fixed and stained as described above with appropriate antibodies.

For RNA-Polymerase II peptide competition experiments, cells were fixed and stained as described above. However, the primary antibody mixtures underwent an extra incubation step prior to being used for staining. The RNA polymerase II phospho S5 antibody was diluted in the blocking solution described above along with 2 ug of either RNA polymerase II CTD repeat

YSPTSPS peptide-phospho S5 (Abcam ab18488) or the same unphosphorylated RNA polymerase II CTD repeat peptide (ab12795). These mixtures were incubated at 4°C for 2 hours while rotating end-over-end. The antibody mixtures were then used to stain cells, and secondary antibodies and mounting were performed as described above.

RNASEH Assay: This assay was performed as described previously (40, 42). U2OS cells were plated on coverslips on day 1, transfected with 50 pmol of various siRNAs on days 2 and 3, transfected on day 4 with either 4ug of pcDNA3 empty vector or pcDNA3 RNASEH1 (43) using Lipofectamine 2000 (Life Technologies Cat. # 11668019), and fixed for immunofluorescent staining 24 hours later on day 5 using 3% paraformaldehyde. Cells were permeabilized using 0.5% Triton X-100 (0.5% Triton X-100, 20mM Hepes pH 7.4, 50mM NaCl, 3mM MgCl2, and 300mM Sucrose dissolved in ddH2O) and then co-stained for γH2AX (Millipore 05-636 at 1:500) and RNASEH1 (Proteintech #15606-1-AP at 1:300). Extra coverslips were stained with either FUS or TDP43 antibodies to assess depletion. Secondary antibodies were Abcam Alexa Fluor 488 anti-rabbit and 594 anti-mouse (Cat. #Ab150077 and Ab150116). Cells were photographed using a Zeiss Axioskop 2 MOT microscope, and the number of nuclei containing 5 or more γH2AX foci was counted for each siRNA with each treatment. The experiment was performed four, separate times; and the average fraction of cells containing 5 or more γH2AX foci from each treatment was calculated from the results of all four experiments. For vector transfected cells, all DAPI positive nuclei were counted and the number of γH2AX foci in every nucleus was assessed. The number of DAPI-positive nuclei containing five or more γH2AX foci compared to the total number of DAPI positive nuclei counted was used to calculate the percentage of cells with 5 or more γH2AX foci for the vector transfected cells. For the RNASEH1 transfected cells, only RNASEH1 positive nuclei were counted and γH2AX foci were assessed in these nuclei. The number of RNASEH1 positive nuclei containing five or more γH2AX foci compared to the total number of RNASEH1 positive nuclei counted was used to calculate the percentage of cells with 5 or more γH2AX foci for the RNASEH1 transfected cells. A minimum of 200 cells was counted for each siRNA treatment for every experiment. Error bars were generated based on the standard deviation between each experiment. p-values assessing the significance of the difference between the vector and RNASEH1 values for each siRNA were generated using a paired two tailed T-test using GraphPad Prism.

Western Blots: After each comet or α-Amanitin sensitivity assay, there was a population of transfected cells that was not plated or used in the assay. These cells were pelleted and used for western blot analysis to assess selected protein depletion phenomena for each of the replicates of the various experiments. Here cells were pelleted, washed with PBS, and lysed in NETN300 lysis buffer (300mM NaCl, 50mM Tris-HCl pH 7.5, 1mMEDTA, 0.5% NP40, 10% Glycerol). Protein concentrations of the lysates were assessed, and the lysates were then diluted to achieve equivalent concentrations using Laemmli running buffer containing β-mercaptoethanol. Equivalent amounts of each sample were loaded onto and electrophoresed through 4-12% Bis-Tris gels, transferred to 0.45um nitrocellulose membranes which were then blocked in 5% milk, and blotted with appropriate primary antibodies for at least one hour or overnight at 4°C. Blots were then incubated with appropriate HRP-conjugated secondary antibodies for 1 hour, washed, and imaged using chemiluminescence reagent and film. Primary and secondary antibodies included Mouse anti-TDP43 (Santa Cruz Cat. # sc-100871), Mouse anti-FUS (Santa Cruz sc-47711), Goat Anti-Mouse light chain HRP conjugate (EMD Millipore Cat. # AP200P), and Mouse anti-tubulin (Sigma Cat. #T-5168).

Results:

Depletion of FUS and TDP43 leads to transcription-stalling agent hypersensitivity

Arrest of transcription by the RNA Polymerase II (RNAPollII) inhibitor, α-Amanitin, leads to an increase in the abundance of γH2AX foci and increased DNA damage likely through transcription fork arrest/collapse, transcription/replication collision, R loop stabilization, and/or exposure of DNA to damaging agents during transcription. If depletion of a protein leads to increased sensitivity to α-Amanitin-induced transcription arrest, this would suggest that the protein of interest is required for prevention or repair of the DNA damage associated with transcription arrest. Indeed, we have previously found that cellular depletion of the tumor suppressor and classic DNA damage repair protein, BRCA1, leads to increased sensitivity to α-Amanitin-driven transcription arrest, and that this sensitivity is due to increased DNA damage (40). In the same work, we detected multiple roles for BRCA1 in the prevention and repair of transcription-associated DNA damage, including in promoting the restart of transcription after UV arrest and preventing/repairing R loop DNA driven damage (40). Thus, we asked whether or not cells depleted of FUS or TDP43 exhibit an increase in α-Amanitin sensitivity.

In these experiments, we transfected cells with either a control siRNA (siGL2) or each of two, different siRNAs targeting each protein (Figure 1A and 1D). Then we tested for sensitivity to α-Amanitin in a colony-forming assay (Figure 1B, C, E, and F). We found that depletion of either FUS or TDP43 led to increased sensitivity to α-Amanitin, suggesting that loss of function of either FUS or TDP43, leads to a defect in the prevention or repair of DNA damage associated with the halting of transcription.

Depletion of FUS and TDP43 leads to increased DNA damage in the setting of transcription arrest

An increased sensitivity to transcription arrest could be due to loss of a variety of FUS and TDP43 functions, including a role in DNA damage prevention or repair. Thus, to test further whether the increased α-Amanitin sensitivity observed in Figure 1 in the setting of FUS and TDP43 depletion was due to increased DNA damage, we performed alkaline comet assays on cells transfected with an siGL2 control and each of the two FUS and two TDP43 siRNAs used in Figure 1 (Figure 2). We chose this assay, because it can recognize both single and double strand breaks in the DNA, either of which is a possible outcome following transcription arrest. We found that depletion of either FUS or TDP43 led to increased DNA damage in the setting of α-Amanitin treatment, suggesting that the increased α-Amanitin sensitivity observed in Figure 1, is due, at least in part, to increased DNA damage, implying that these proteins are necessary to suppress or repair DNA damage in the setting of transcription arrest.

FUS localizes to sites of transcription-associated DNA damage with another classic DNA damage repair protein

The finding that FUS participates in the prevention or repair of transcription-associated DNA damage is consistent with the prior finding that FUS localizes to DSBs induced by a UV laser (24-26). In turn, the latter is consistent with two functional possibilities: a) that FUS participates in the repair of DSBs, per se, and b) that it localizes to breaks located near sites of transcription-associated DNA damage. In support of possibility b, FUS functions in both the soluble nuclear and chromatin fraction, and in the chromatin fraction it interacts with the C terminal domain of RNA Pol II and modulates its phosphorylation on Serine 2 to help regulate transcription of specific genes (44, 45). FUS is also known to co-localize with active RNA Pol II in undamaged cells where it is thought to aid in transcription of specific genes, for RNA Pol II Serine 2 phosphorylation was altered at the sites of specific genes in fibroblasts from patients

with FUS mutations (46). Given its physical and functional interaction with RNA Pol II and its localization to sites of DSBs, it is likely that FUS functions in transcription-associated DNA damage.

To assess more specifically whether FUS localizes at sites of transcription-associated DNA damage, we searched for FUS in UV-induced DNA damage foci that are associated with transcription arrest (40). We showed previously that UV damage induces active RNAPolII-containing foci that co-localize with DNA damage markers such as phosphorylated-RPA, γH2AX, and BRCA1 (40). This suggests that these foci are active sites of transcription-associated DNA damage repair. Thus, we searched for FUS in post-UV RNAPolII foci using an aggressive methanol-acetic acid fixation method to remove the soluble nuclear fraction and better reveal the chromatin fraction which is known to interact with RNA Pol II. The underlying hypothesis was that FUS would localize to these sites to help regulate or repair transcription-associated DNA damage given its known links to RNA Pol II and functions in DNA damage repair.

First we observed that our FUS and RNAPolII antibodies were target-specific (Figure 3). We then found that, after UV damage, there was a significant increase in the number of cells with co-localizing FUS and active RNAPolII foci compared to the untreated control, suggesting that FUS localizes to sites of active transcription after UV damage to either prevent or repair DNA damage at these sites (Figure 4A).

To test further whether there was DNA damage at these post-UV RNAPolII sites, we co-stained for FUS and the DNA damage markers γH2AX (Figure 4B), phosphorylated RPA (Figure 5A), and BRCA1 (Figure 5B). We chose these markers because we have previously shown that a significant fraction of post-UV BRCA1 foci overlap with active RNAPolII, γH2AX, and phosphorylated RPA-containing foci, suggesting that a significant number of the active RNAPolII foci contain γH2AX and phosphorylated RPA and thus transcription-associated DNA damage (40). We detected increased nuclear co-localization of FUS with γH2AX (Figure 4B), phosphorylated RPA (Figure 5A), and BRCA1 (Figure 5B) after UV damage, suggesting that FUS localizes at transcription-associated DNA damage sites. This implies that, after UV damage-induced transcription arrest, FUS localizes to genomic sites where active transcription has been arrested by DNA damage, and it does so together with BRCA1. Presumably, its role is to participate in the repair of this damage through its HR or NHEJ functions and/or to prevent the

development of additional damage e.g. by stabilizing and/or repairing any stalled/collapsed transcribed DNA. FUS also co-localizes with γH2AX (Figure 4B), pRPA (Figure 5A), and BRCA1 (Figure 5B) in cells that were not ectopically damaged, suggesting that its baseline function in cycling cells includes some form of indigenous DNA damage prevention or repair.

TDP43 localizes to sites of transcription-associated DNA damage together with FUS

With the knowledge that TDP43 depletion, like that of FUS depletion, leads to increased sensitivity to α-Amanitin and that FUS localizes to sites of post-UV, transcription associated DNA damage, we asked whether or not TDP43 also concentrates at these DNA damage sites. We first determined that our TDP43 antibody was specific (Figure 6) and then assessed whether or not TDP43 also co-localizes with active RNAPolII after UV damage. Indeed, more cells revealed co-localizing TDP43 and active RNAPolII foci after UV damage than in an undamaged state (Figure 7A). This suggests that TDP43, like FUS and BRCA1, localizes to sites of transcription associated DNA damage and, in that context, likely participates in either the prevention of further damage or in DNA damage repair.

To test further whether TDP43 also localizes to sites of transcription-associated DNA damage, we assessed whether or not TDP43 co-localized with γH2AX and phosphorylated RPA after UV treatment. The data revealed that TDP43 co-localized with γH2AX and phosphorylated RPA in an increased percentage of cells post-UV (Figures 7B and 8A). Interestingly, even in the setting of no ectopically induced DNA damage, TDP43 co-localized with γH2AX (Figure 7B) and phosphorylated RPA (Figure 8A) suggesting that it functions in preventing or repairing spontaneously arising DNA damage as might occur when spontaneously arising defects in baseline transcription beget DNA damage.

Finally, we tested whether or not FUS and TDP43 co-localize post-UV. We found that at baseline, FUS and TDP43 foci overlap significantly, implying that they reflect certain common molecular outcomes (Figure 8B), as suggested by their known functional profiles (11, 12) and results reported here (Figures 1, 2, and 9). FUS and TDP43 co-localization also increased after UV treatment, implying that they both participate, possibly even together, in dealing with the same forms of transcription-associated DNA damage. Since FUS significantly co-localized with BRCA1, and FUS and TDP43 also significantly co-localized, it is likely that TDP43 also co-localizes with BRCA1 in some DNA damage foci.

FUS and TDP43 participate in either the prevention or repair of R-loop associated DNA damage

There are multiple forms of transcription-associated DNA damage in which FUS and TDP43 might participate, as described previously. A particularly appealing form is DNA damage associated with R-loops. R-loops are normal physiologic structures generated during transcription that consist of a) the DNA-RNA hybrid generated by the transcribed DNA strand annealing to the nascent RNA transcript and b) the looped-out non-transcribed strand. Normally, they are resolved with the help of multiple proteins, including one protein linked to familial ALS, SETX (19, 20). However, when they are not resolved, due to loss of function of one of multiple proteins, unrepaired single stranded breaks on the non-transcribed strand that evolve to DSBs can result and lead to cell death (19, 20, 43). The idea that FUS and/or TDP43 is involved in the prevention or repair of R-loop associated DNA damage is appealing since these proteins appear to participate in DNA damage prevention or repair even in the setting of no exogenous damage (Figures 4B and 7B). Moreover, other familial ALS proteins are involved in the prevention/repair of this type of damage (19, 20), and another DNA damage protein, BRCA1, that localizes to the same post-UV RNAPolII DNA damage foci has also been found to participate in the prevention and/or repair of R-loop associated DNA damage (40, 47).

Thus, we tested whether or not FUS and/or TDP43 participate in the prevention or repair of R-loop-associated DNA damage by searching for a decrease in DNA damage in the setting of FUS or TDP43 depletion when RNASEH1 is exogenously overexpressed. RNASEH1 is an enzyme that specifically digests DNA-RNA hybrids such as those that give rise to R-loops (43). Assessing DNA damage markers in the setting of gene-specific depletion and RNASEH1 overexpression has previously been used to determine whether or not proteins are involved in R-loop-associated DNA damage prevention or repair (40, 42).

We assessed the results of RNASEH1 overexpression and antibody specificity (Figure 9A) and also FUS and TDP43 depletion using the IF-associated fixation method necessary for this assay (Figures 9B and 9C). Both proved to be satisfactory. We then co-stained cells transfected with a control siRNA or FUS- or TDP43- specific siRNAs and co-transfected with empty vector or an RNASEH1-encoding vector for the DNA damage marker, γH2AX, as well as for RNASEH1 expression. For the empty vector treated cells, all DAPI positive nuclei were counted and γH2AX foci in all nuclei were assessed. In each experiment, the percentage of

vector-transfected cells for each siRNA that contained 5 or more γH2AX foci was calculated, i.e. the number of DAPI positive nuclei containing five or more γH2AX foci was divided by the total number of DAPI nuclei counted. For RNASEH1-transfected cells, only RNASEH1-positive nuclei were counted and γH2AX foci were only assessed in RNASEH1-positive nuclei. For each siRNA employed, the percentage of RNASEH1-transfected cells that contained 5 or more γH2AX foci was calculated from the number of RNASEH1 positive nuclei with five or more γH2AX foci divided by the total number of RNASEH1 nuclei present.

For the control siRNA, there was no significant difference in the fraction of cells containing 5 or more γH2AX foci between vector and RNASEH1 transfected cells (Figure 9D). However, in multiple replicate experiments there was an incomplete but statistically significant decrease in cells containing increased γH2AX foci in cells transfected with RNASEH1 compared to vector in both siFUS- and siTDP43- transfected cells (Figure 9D). This suggests that part of the DNA damage confronted by both FUS and TDP43, like the other familial ALS protein SETX, was R-loop-associated.

iPSC derived wildtype motor neurons exhibit FUS co-localization with UV induced RNA Polymerase foci

All of the experiments in Figures 1-9 were performed in U2OS cells which are cycling cells derived from an osteosarcoma. There could be mechanistic differences between this rapidly cycling cancer cell line and motor neurons, especially with respect to DNA damage recognition and repair. Therefore, it will be important in future experiments to replicate some or all of this data in motor neurons which can likely be accomplished using induced pluripotent stem cell (iPSC) derived motor neurons. In an initial pilot experiment on mature wildtype iPSC derived motor neurons treated with either 0J or 25J, FUS co-localized with UV-induced RNA Pol II pS5 foci 4 hours after UV treatment (Figure 10), indicating that perhaps the mechanistic role of FUS at sites of transcription-associated DNA damage is the same in G0 motor neurons as it is in cycling cells. More extensive staining and quantitation will be needed to verify this possibility, and this is ongoing.

Discussion, Conclusions, and Suggestions for Future Work:

The combined α-Amanitin sensitivity, comet, and immunofluorescence analysis results in this study suggest that both FUS and TDP43 are necessary for the prevention or repair of transcription-associated DNA damage, including R-loop induced DNA damage, and that they

localize to nuclear sites laden with this type of DNA damage for these reasons (Figures 1-9). With verification of these results in iPSC derived motor neurons, which is currently ongoing, these findings might be consistent with the hypothesis that there is a role for DNA damage prevention and/or repair in suppressing both familial and sporadic ALS. More specifically, this would suggest that at least some of the relevant DNA damage is a product of defective transcription and/or RNA processing.

Although human tissue studies and mouse models have not yet conclusively shown that markers of DNA damage coincide with markers of cell death in motor neurons (25, 48), the possibility that transcription-associated DNA damage contributes to motor neuron cell death in ALS remains. Based on our work and the work of others, it is reasonable to develop a model of ALS pathogenesis in which various ALS proteins, such as FUS and TDP43, prevent or repair the various forms of transcription-associated DNA damage described previously, such as R-loop-associated damage. Perhaps through stable formation of hydrogel or fibrous states (8, 9), some of these ALS related proteins with LC domains like FUS, TDP43, EWSR1, or TAF15 incur loss of an important nuclear function related to transcription-associated DNA damage such as in stabilizing damaged transcription structures and recruiting repair machinery or participating in the repair itself, which would result in abnormally high numbers of stable R loops, stalled transcription machinery, or stably open DNA all of which would be susceptible to DNA damage that could eventually mature into DSBs. In non-proliferating neurons, DSBs are repaired by error-prone NHEJ machinery (49). Over time these sites may accumulate mutations, genome, rearrangements, and/or chromatid breaks. Enough genomic disorder might accumulate to result in cell death, the major feature of ALS. Determining whether some forms of ALS are driven by ongoing transcription-associated DNA damage will be an important aspect of future work in the field.

Based on the results described here and the work of others, there is already support for this method of ALS pathogenesis, especially with respect to FUS related cases. Our results fit with observations that FUS localizes to sites of UV-laser induced DNA damage and support a role for FUS in DNA damage repair (24-26). Previous work has shown that FUS is recruited to DSBs where it forms a liquid phase compartment and where is important in D loop formation in the initial phase of HR and in recruiting repair proteins to DSBs (9, 25, 33). In those studies, FUS was shown to localize to these linear arrays of DSBs in a PARP dependent manner prior to

the localization of markers of DNA damage such as γH2AX or proteins involved in the repair of DSBs such as NBS1 or Ku70 (24, 25, 27). In addition, the authors found that localization of these DNA damage markers and repair proteins to DSBs decreased in the setting of FUS depletion, suggesting that FUS function is necessary to stabilize the DNA damage structure, prepare it for repair, or induce modifications needed to recruit these other proteins (25). Our finding that FUS localizes to sites of transcription-associated DNA damage, co-localizes with markers of DNA damage without any exogenous damage, and participates in the prevention/repair of R-loop induced DNA damage fits with these findings and supports the notion that FUS functions, at least in part, in transcription-associated DNA damage.

Our findings that FUS localizes to sites of transcription-associated DNA damage after enrichment for such damage by UV treatment suggest that when FUS localizes to DNA damage in untreated cells, it is likely localizing to sites of spontaneously arising, transcription-associated DNA damage, in some cases R-loop associated damage. This further suggests that, at baseline, FUS is recruited to DNA damage structures and once there, participates in the repair process directly and/or marks or stabilizes the damaged structures for repair. FUS may be one of the earliest proteins to arrive at these sites to stabilize an 'open' transcription structure, for others have shown that FUS forms liquid compartments at sites of DNA damage in cells (9) and that without FUS recruitment other DNA damage repair proteins like NBS1 or Ku70 operate inefficiently (25). In contrast, instead of being recruited, perhaps FUS is already present, processing along the DNA with the transcription machinery to hold the damaged DNA in place for repair, if necessary. Indeed, FUS is known to interact with active RNA Pol II and regulate its phosphorylation (44-46). This interaction was thought to be aimed at regulating the transcription of specific genes, and, perhaps, that regulation also operates in the setting of DNA damage, possibly meaning that FUS processes along with RNA Pol II and helps repair damage after a collision or collapse to ensure continued transcription and mRNA processing, or to block the transcription of damaged DNA (46). Further work will be necessary to assess these possibilities.

We also find that TDP43, like FUS, plays a role in transcription-associated DNA damage prevention and repair, in particular in R-loop associated DNA damage, and may share with FUS its above-noted role in stabilizing transcription-associated damage or aiding in its repair (Figures 7-8). TDP43 and FUS significantly co-localize prior to DNA damage and co-localize even more so after DNA damage suggesting multiple shared functions for these proteins (Figure 8B). It is

interesting that FUS and TDP43 co-localize in foci in the absence of exogenous mutagen exposures and of γH2AX. Some of these spontaneously arising foci also co-localized with γH2AX and pRPA, again suggesting that one of their baseline functions may be in DNA damage repair or prevention and that perhaps the co-localizing FUS and TDP43 at sites that lack γH2AX or pRPA are 'built in' structures that pre-exist to deal with transcription-associated DNA damage whether or not there is any present. In addition, FUS and TDP43 share yet other functions (11, 12). Given these shared functions, it is likely that loss of function of either protein, either through mutation or aberrant cytoplasmic localization in the wild type setting, contributes to ALS pathogenesis through the DNA damage prevention/repair mechanism described above. It is possible that some of the multiple other RNA binding proteins linked to ALS through genetic studies, including EWSR1 and TAF15, may also play a role in the mechanism described above and contribute to ALS in a similar DNA damage driven mechanism (1). Further work will be needed to assess these possibilities.

Multiple current and past ALS-related studies on human neural tissue were performed on autopsy material obtained long after the central activity of the disease-producing process has likely ended, making it difficult to identify abnormal events that contribute to an emerging disease-producing state. In addition, the mouse models used in ALS studies have mostly failed to mimic both classic human ALS histology and its associated neurologic findings in the same model, making studies of the disease mechanism in these animals difficult to interpret (10). Studies of neural tissue from mouse models that actively mimic the combined histologic findings and related neurologic phenotypes during the process of disease emergence will be necessary to better determine whether or not transcription associated DNA-damage is associated with motor neuron cell death during the path to ALS.

Specific to the work detailed in this thesis, key future experiments that are already ongoing will be to determine whether it is possible to replicate some of the data in Figures 1-9 in iPSC derived motor neurons from healthy and ALS patients. In addition, demonstrating that these motor neurons undergo cell death as a result of this damage will be critical in determining whether or not loss of this particular function of FUS and TDP43, amongst other ALS related proteins, is important in ALS pathogenesis. Replicating the above-noted experiments in U2OS cells and motor neurons for TAF15 and EWSR1, which are known to be involved in DNA damage (16), would be another important step, as would testing other ALS linked proteins for

this same function. A better understanding of the exact molecular roles of FUS and TDP43, along with other ALS-related proteins, in transcription-associated DNA damage will also be needed to aid in this process.

Moreover, defining which of their molecular binding partners aid in these roles will be critical in determining whether the transcription-associated DNA damage control function of FUS and TDP43 is lost and thereby contributes to the pathogenesis of ALS. A better understanding of this function could also aid in conceiving of and generating new biomarkers of the disease that aid in making an ALS diagnosis and in tracking disease progression.

Summary:

In summary, this work suggests that the fALS proteins FUS and TDP43 are involved in the prevention or repair of transcription-associated DNA damage. In support of this conclusion, upon depletion of these proteins, cells become sensitive to transcription arresting agents at least in part due to increased amounts of DNA damage suggesting that these proteins are required for cell survival after DNA damage linked to transcription failure. In addition, after UV treatment, which arrests transcription, both FUS and TDP43 co-localized with active RNA Polymerase II in distinct foci which also contain markers of DNA damage including, BRCA1, γH2AX, and pRPA. This suggests that these proteins play a role in repairing or preventing DNA damage at these sites of arrested transcription. FUS and TDP43 co-localized with each before UV treatment and in increasing numbers of foci after UV treatment suggesting a possible shared role for these proteins at these UV-arrested transcription sites and possibly endogenous sites of transcription-associated and non-associated DNA damage. Finally, among the many possible functions in transcription-associated DNA damage, FUS and TDP43 play a role in the prevention or repair of DNA damage caused by R-loop stabilization. Further work will be necessary to understand the exact mechanism of FUS and TDP43 involvement at these sites and whether or not this is the function lost in the pathogenesis of at least some subtypes of ALS.

Funding Information: SJH was funded initially by DOD BCRP Fellowship W81XWH-08-1-0748 and subsequently by NCI Fellowship 1F30CA167895-01. SJH, SL, and DML were funded by grants from the ALS Therapy Alliance, HNDC Neurodegenerative Disease Pilot Study Grants Program, and the Murray Winston Foundation awarded to DML and SJH.

Acknowledgements: We wish to thank Drs. Merit Cudkowicz and Matthew Frosch for valuable discussions and help, and Drs. Kevin Eggan and Daniel Mordes for providing motor neurons and

helpful discussion. SJH conceived of the project, and DML mentored SJH in its design and execution. SJH performed all experiments and analyzed all data with technical assistance in the performance of the experiments in Figure 1 from SL. SJH wrote the thesis with review by DML.

References:

1. Marangi G, Traynor BJ. Genetic causes of amyotrophic lateral sclerosis: new genetic analysis methodologies entailing new opportunities and challenges. Brain Res. 2015 May 14;1607:75-93.
2. Neumann M, Sampathu DM, Kwong LK, Truax AC, Micsenyi MC, Chou TT, et al. Ubiquitinated TDP-43 in frontotemporal lobar degeneration and amyotrophic lateral sclerosis. Science. 2006 Oct 6;314(5796):130-3.
3. Kwiatkowski TJ, Jr., Bosco DA, Leclerc AL, Tamrazian E, Vanderburg CR, Russ C, et al. Mutations in the FUS/TLS gene on chromosome 16 cause familial amyotrophic lateral sclerosis. Science. 2009 Feb 27;323(5918):1205-8.
4. Lagier-Tourenne C, Polymenidou M, Cleveland DW. TDP-43 and FUS/TLS: emerging roles in RNA processing and neurodegeneration. Hum Mol Genet. 2010 Apr 15;19(R1):R46-64.
5. Kato M, Han TW, Xie S, Shi K, Du X, Wu LC, et al. Cell-free formation of RNA granules: low complexity sequence domains form dynamic fibers within hydrogels. Cell. 2012 May 11;149(4):753-67.
6. Malinovska L, Kroschwald S, Alberti S. Protein disorder, prion propensities, and self-organizing macromolecular collectives. Biochim Biophys Acta. 2013 May;1834(5):918-31.
7. Elbaum-Garfinkle S, Brangwynne CP. Liquids, Fibers, and Gels: The Many Phases of Neurodegeneration. Dev Cell. 2015 Dec 7;35(5):531-2.
8. Murakami T, Qamar S, Lin JQ, Schierle GS, Rees E, Miyashita A, et al. ALS/FTD Mutation-Induced Phase Transition of FUS Liquid Droplets and Reversible Hydrogels into Irreversible Hydrogels Impairs RNP Granule Function. Neuron. 2015 Nov 18;88(4):678-90.
9. Patel A, Lee HO, Jawerth S, Jahnel M, Hein MY, Stoynov S, et al. A Liquid-to-Solid Phase Transition of the ALS Protein FUS Accelerated by Disease Mutation. Cell. 2015;162(5):1066-77.
10. Ittner LM, Halliday GM, Kril JJ, Gotz J, Hodges JR, Kiernan MC. FTD and ALS--translating mouse studies into clinical trials. Nat Rev Neurol. 2015 Jun;11(6):360-6.

11. Janssens J, Van Broeckhoven C. Pathological mechanisms underlying TDP-43 driven neurodegeneration in FTLD-ALS spectrum disorders. Hum Mol Genet. 2013 Oct 15;22(R1):R77-87.
12. Sama RR, Ward CL, Bosco DA. Functions of FUS/TLS from DNA repair to stress response: implications for ALS. ASN Neuro. 2014;6(4).
13. Aguilera A, Garcia-Muse T. R loops: from transcription byproducts to threats to genome stability. Mol Cell. 2012 Apr 27;46(2):115-24.
14. Skourti-Stathaki K, Proudfoot NJ. A double-edged sword: R loops as threats to genome integrity and powerful regulators of gene expression. Genes Dev. 2014 Jul 1;28(13):1384-96.
15. Paulsen RD, Soni DV, Wollman R, Hahn AT, Yee MC, Guan A, et al. A genome-wide siRNA screen reveals diverse cellular processes and pathways that mediate genome stability. Mol Cell. 2009 Jul 31;35(2):228-39.
16. Izhar L, Adamson B, Ciccia A, Lewis J, Pontano-Vaites L, Leng Y, et al. A Systematic Analysis of Factors Localized to Damaged Chromatin Reveals PARP-Dependent Recruitment of Transcription Factors. Cell Rep. 2015 Jun 9;11(9):1486-500.
17. Helmrich A, Ballarino M, Nudler E, Tora L. Transcription-replication encounters, consequences and genomic instability. Nat Struct Mol Biol. 2013 Apr;20(4):412-8.
18. Zeman MK, Cimprich KA. Causes and consequences of replication stress. Nat Cell Biol. 2014 Jan;16(1):2-9.
19. Mischo HE, Gomez-Gonzalez B, Grzechnik P, Rondon AG, Wei W, Steinmetz L, et al. Yeast Sen1 helicase protects the genome from transcription-associated instability. Mol Cell. 2011 Jan 7;41(1):21-32.
20. Skourti-Stathaki K, Proudfoot NJ, Gromak N. Human senataxin resolves RNA/DNA hybrids formed at transcriptional pause sites to promote Xrn2-dependent termination. Mol Cell. 2011 Jun 24;42(6):794-805.
21. Yuce O, West SC. Senataxin, defective in the neurodegenerative disorder ataxia with oculomotor apraxia 2, lies at the interface of transcription and the DNA damage response. Mol Cell Biol. 2013 Jan;33(2):406-17.
22. Yeo AJ, Becherel OJ, Luff JE, Cullen JK, Wongsurawat T, Jenjaroenpun P, et al. R-loops in proliferating cells but not in the brain: implications for AOA2 and other autosomal recessive ataxias. PLoS One. 2014;9(3):e90219.

23. Kovar H. Dr. Jekyll and Mr. Hyde: The Two Faces of the FUS/EWS/TAF15 Protein Family. Sarcoma. 2011;2011:837474.
24. Mastrocola AS, Kim SH, Trinh AT, Rodenkirch LA, Tibbetts RS. The RNA-binding protein fused in sarcoma (FUS) functions downstream of poly(ADP-ribose) polymerase (PARP) in response to DNA damage. J Biol Chem. 2013 Aug 23;288(34):24731-41.
25. Wang WY, Pan L, Su SC, Quinn EJ, Sasaki M, Jimenez JC, et al. Interaction of FUS and HDAC1 regulates DNA damage response and repair in neurons. Nat Neurosci. 2013 Oct;16(10):1383-91.
26. Rulten SL, Rotheray A, Green RL, Grundy GJ, Moore DA, Gomez-Herreros F, et al. PARP-1 dependent recruitment of the amyotrophic lateral sclerosis-associated protein FUS/TLS to sites of oxidative DNA damage. Nucleic Acids Res. 2014 Jan;42(1):307-14.
27. Jungmichel S, Rosenthal F, Altmeyer M, Lukas J, Hottiger MO, Nielsen ML. Proteome-wide identification of poly(ADP-Ribosyl)ation targets in different genotoxic stress responses. Mol Cell. 2013 Oct 24;52(2):272-85.
28. Hurov KE, Cotta-Ramusino C, Elledge SJ. A genetic screen identifies the Triple T complex required for DNA damage signaling and ATM and ATR stability. Genes Dev. 2010 Sep 1;24(17):1939-50.
29. Paronetto MP, Minana B, Valcarcel J. The Ewing sarcoma protein regulates DNA damage-induced alternative splicing. Mol Cell. 2011 Aug 5;43(3):353-68.
30. Akhmedov AT, Bertrand P, Corteggiani E, Lopez BS. Characterization of two nuclear mammalian homologous DNA-pairing activities that do not require associated exonuclease activity. Proc Natl Acad Sci U S A. 1995 Feb 28;92(5):1729-33.
31. Baechtold H, Kuroda M, Sok J, Ron D, Lopez BS, Akhmedov AT. Human 75-kDa DNA-pairing protein is identical to the pro-oncoprotein TLS/FUS and is able to promote D-loop formation. J Biol Chem. 1999 Nov 26;274(48):34337-42.
32. Liu X, Niu C, Ren J, Zhang J, Xie X, Zhu H, et al. The RRM domain of human fused in sarcoma protein reveals a non-canonical nucleic acid binding site. Biochim Biophys Acta. 2013 Feb;1832(2):375-85.
33. Ceccaldi R, Rondinelli B, D'Andrea AD. Repair Pathway Choices and Consequences at the Double-Strand Break. Trends Cell Biol. 2016 Jan;26(1):52-64.

34. Dobbin MM, Madabhushi R, Pan L, Chen Y, Kim D, Gao J, et al. SIRT1 collaborates with ATM and HDAC1 to maintain genomic stability in neurons. Nat Neurosci. 2013 Aug;16(8):1008-15.
35. Pasinelli P, Brown RH. Molecular biology of amyotrophic lateral sclerosis: insights from genetics. Nat Rev Neurosci. 2006 Sep;7(9):710-23.
36. Pan L, Penney J, Tsai LH. Chromatin regulation of DNA damage repair and genome integrity in the central nervous system. J Mol Biol. 2014 Oct 9;426(20):3376-88.
37. Hill SJ, Landini, S., and Livingston, D.M. Familial ALS proteins function in prevention/repair of transcription-associated DNA damage. Submitted. 2015.
38. Amoroso MW, Croft GF, Williams DJ, O'Keeffe S, Carrasco MA, Davis AR, et al. Accelerated high-yield generation of limb-innervating motor neurons from human stem cells. J Neurosci. 2013 Jan 9;33(2):574-86.
39. Espinosa JM, Verdun RE, Emerson BM. p53 functions through stress- and promoter-specific recruitment of transcription initiation components before and after DNA damage. Mol Cell. 2003 Oct;12(4):1015-27.
40. Hill SJ, Rolland T, Adelmant G, Xia X, Owen MS, Dricot A, et al. Systematic screening reveals a role for BRCA1 in the response to transcription-associated DNA damage. Genes Dev. 2014 Sep 1;28(17):1957-75.
41. Scully R, Ganesan S, Brown M, De Caprio JA, Cannistra SA, Feunteun J, et al. Location of BRCA1 in human breast and ovarian cancer cells. Science. 1996 Apr 5;272(5258):123-6.
42. Herrera-Moyano E, Mergui X, Garcia-Rubio ML, Barroso S, Aguilera A. The yeast and human FACT chromatin-reorganizing complexes solve R-loop-mediated transcription-replication conflicts. Genes Dev. 2014 Apr 1;28(7):735-48.
43. Li X, Manley JL. Inactivation of the SR protein splicing factor ASF/SF2 results in genomic instability. Cell. 2005 Aug 12;122(3):365-78.
44. Schwartz JC, Ebmeier CC, Podell ER, Heimiller J, Taatjes DJ, Cech TR. FUS binds the CTD of RNA polymerase II and regulates its phosphorylation at Ser2. Genes Dev. 2012 Dec 15;26(24):2690-5.
45. Yang L, Gal J, Chen J, Zhu H. Self-assembled FUS binds active chromatin and regulates gene transcription. Proc Natl Acad Sci U S A. 2014 Dec 16;111(50):17809-14.

46. Schwartz JC, Podell ER, Han SS, Berry JD, Eggan KC, Cech TR. FUS is sequestered in nuclear aggregates in ALS patient fibroblasts. Mol Biol Cell. 2014 Sep 1;25(17):2571-8.
47. Bhatia V, Barroso SI, Garcia-Rubio ML, Tumini E, Herrera-Moyano E, Aguilera A. BRCA2 prevents R-loop accumulation and associates with TREX-2 mRNA export factor PCID2. Nature. 2014 Jul 17;511(7509):362-5.
48. Qiu H, Lee S, Shang Y, Wang WY, Au KF, Kamiya S, et al. ALS-associated mutation FUS-R521C causes DNA damage and RNA splicing defects. J Clin Invest. 2014 Mar;124(3):981-99.
49. Sharma S. Age-related nonhomologous end joining activity in rat neurons. Brain Res Bull. 2007 Jun 15;73(1-3):48-54.

Figure 1

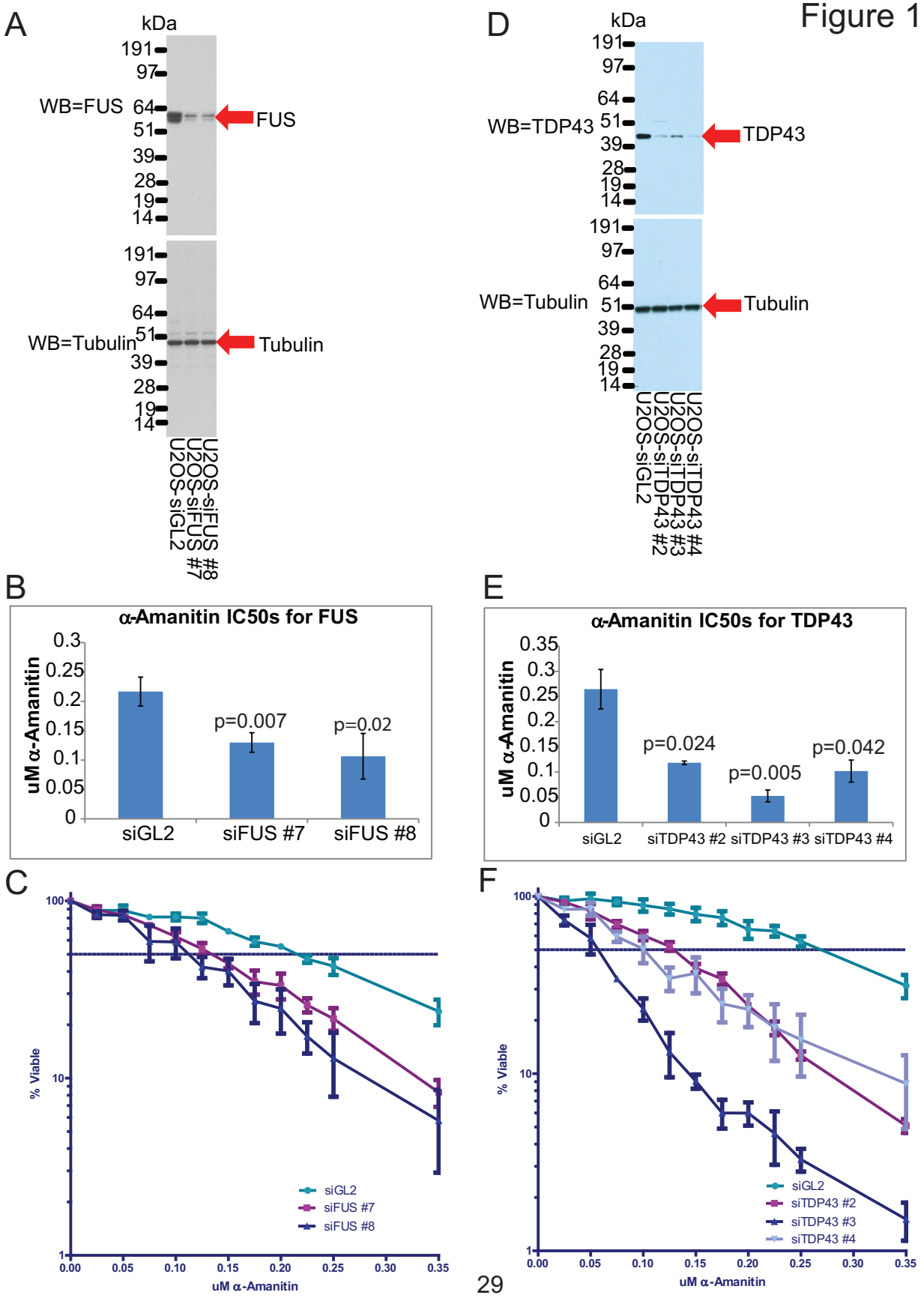
A
kDa
191
97
64
51
39
28
19
14
WB=FUS
FUS
WB=Tubulin
Tubulin
U2OS-siGL2
U2OS-siFUS #7
U2OS-siFUS #8
D
WB=TDP43
TDP43
U2OS-siGL2
U2OS-siTDP43 #2
U2OS-siTDP43 #3
U2OS-siTDP43 #4
B
α-Amanitin IC50s for FUS
uM α-Amanitin
p=0.007
p=0.02
siGL2
siFUS #7
siFUS #8
E
α-Amanitin IC50s for TDP43
p=0.024
p=0.005
p=0.042
siGL2
siTDP43 #2
siTDP43 #3
siTDP43 #4
C
% Viable
uM α-Amanitin
F

Figure 1-Depletion of fALS proteins leads to increased sensitivity to a transcription stalling agent: A) Western blot demonstrating that FUS siRNAs deplete FUS protein. The blot in the top panel shows FUS protein levels in U2OS cells transfected with a control siRNA and the two FUS siRNAs that were also used in experiments depicted in panels 1B and 1C. This blot was stripped and stained with anti-tubulin antibody, which served as a loading control, which is shown in the bottom panel. **B)** U2OS cells were transfected with the siRNAs used in panel 1A (the siGL2 control and two FUS specific siRNAs), plated at a sufficient density for colony formation, and treated with varying doses of the transcription inhibiting agent α-Amanitin for 24 hours, at which point the media was removed and replaced with fresh non drug-containing media. One week later, the cells were stained with crystal violet solution and the colonies were counted. Dose response curves were generated from these counts, and a non-linear regression curve was fit to the dose response curves in GraphPad Prism in order to calculate the IC50 for each, individual repetition of the experiment performed with each siRNA. The experiment was repeated three separate times for each siRNA. The average IC50 from the three repetitions of the experiment for each siRNA is shown in the bar graph, with the error bars representing the standard deviation between the IC50s. The p-values above the siFUS bars represent the significance of the difference between the siGL2 IC50 and each siFUS IC50 calculated using a paired, two-tailed t-test in GraphPad Prism. **C)** Average dose response curves for the three repetitions of the colony forming experiments described in 1B. The error bars at each dose represent the standard error of the mean (SEM) between the three repetitions of the experiment for each siRNA. **D)** Western blot demonstrating that the three TDP43 siRNAs each deplete TDP43 protein when compared to the siGL2 (firefly luciferase) control. The blot in the top panel shows TDP43 protein levels in U2OS cells transfected with a control siRNA or three TDP43 siRNAs used in the experiments depicted in panels 1E and 1F. This blot was stripped and stained with tubulin as a loading control (see bottom panel). **E)** U2OS cells were transfected with the siRNAs used in panel 1D (siGL2 control and three TDP43-specific siRNAs), plated at a sufficient density for colony formation, and treated with varying doses of α-Amanitin for 24 hours, at which point the media was removed and replaced with fresh non drug-containing media. One week later, the cells were stained with crystal violet solution, and the colonies were counted. Dose response curves were generated from these results, and the data was analyzed as in experiments depicted in Figures 1B and 1C. The p-values above the siTDP43 bars represent the significance of the difference

between the siGL2 IC50 and each siTDP43 IC50 calculated using a paired, two-tailed t-test in GraphPad Prism. **F)** Average dose response curves from the three replicates of the colony formation experiments described in 1E. The error bars at each dose represent the standard error of the mean (SEM) between the three repetitions of the experiment performed with each siRNA.

Figure 2

A

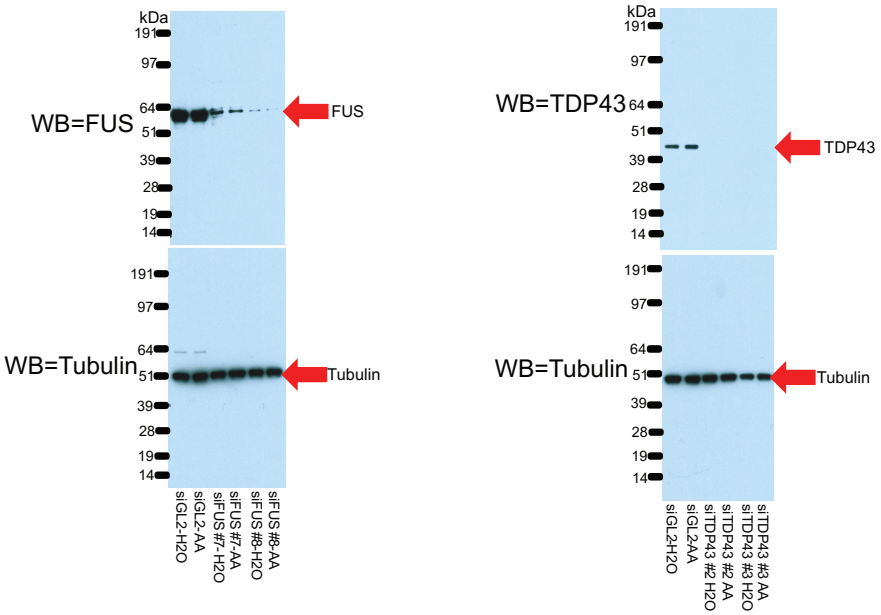
kDa
191
97
64
51
39
28
19
14
WB=FUS
FUS
WB=Tubulin
Tubulin
siGL2-H2O
siGL2-AA
siFUS #7-H2O
siFUS #7-AA
siFUS #8-H2O
siFUS #8-AA
WB=TDP43
TDP43
siTDP43 #2 H2O
siTDP43 #2 AA
siTDP43 #3 H2O
siTDP43 #3 AA

B

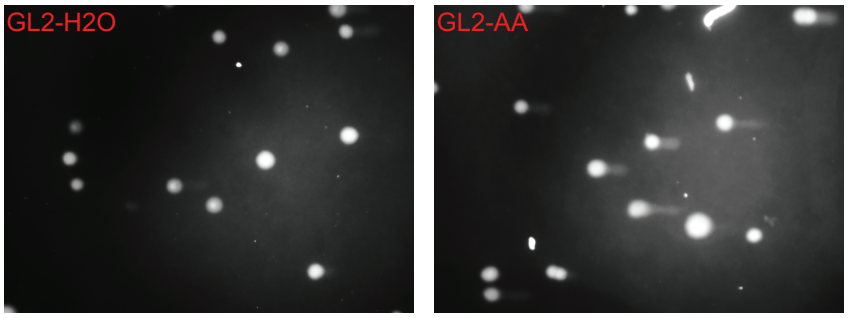
GL2-H2O
GL2-AA

C

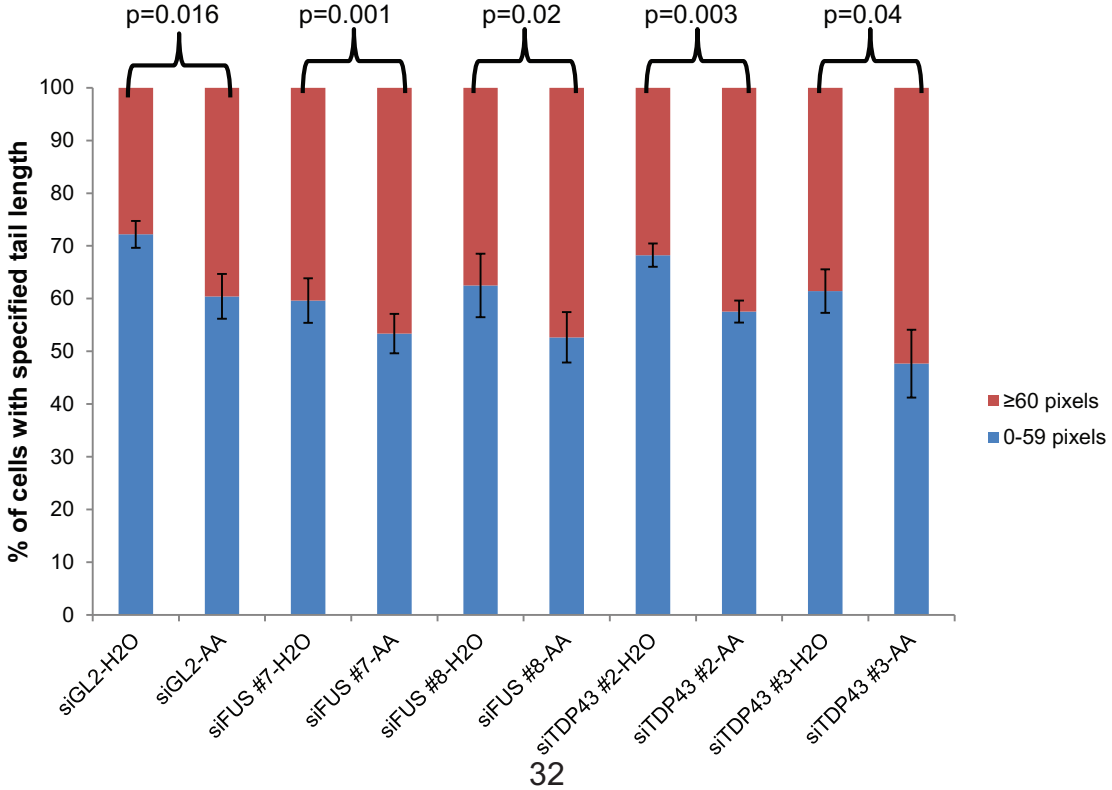
p=0.016
p=0.001
p=0.02
p=0.003
p=0.04
% of cells with specified tail length
100
90
80
70
60
50
40
30
20
10
0
siGL2-H2O
siGL2-AA
siFUS #7-H2O
siFUS #7-AA
siFUS #8-H2O
siFUS #8-AA
siTDP43 #2-H2O
siTDP43 #2-AA
siTDP43 #3-H2O
siTDP43 #3-AA
≥60 pixels
0-59 pixels

Figure 2-Depletion of fALS proteins leads to increased DNA damage accompanying transcription arrest: A) Western blot demonstrating that the FUS and TDP43 siRNAs deplete each protein in the setting of H2O or α-Amanitin (AA) exposure. The blot in the top panel depicts either FUS (left top) or TDP43 (right top) protein levels in U2OS cells transfected with a control siRNA and the two FUS or TDP43 siRNAs and then treated with H2O or AA from one of the four repeat experiments averaged in panel 2C. These blots were stripped and stained with tubulin as a loading control which is shown in the bottom panels. **B)** U2OS cells were transfected with either a control siRNA (siGL2) or siRNAs targeting fALS genes of interest, treated with a toxic dose of α-Amanitin or an equivalent amount of doubly distilled H2O (H2O) for 24 hours, and then analyzed by comet assay to determine the amount of DNA damage present. Tail length was used as a measure of DNA damage. Increased tail length corresponds to increased DNA damage. Representative photos of U2OS cells transfected with siGL2 used with each treatment are shown here. The brightness and contrast were both increased by 40% in all photos using PowerPoint. **C)** 60 pixels was set as a threshold for denoting a culture as demonstrating meaningful DNA damage, and the average percentage of cells with tail lengths greater (red) or less (blue) than 60 pixels for each siRNA with each treatment is shown from four separate experiments. The error bars represent the standard deviation between the three experiments. The p-value denoting the significance of the difference between the percentages greater than 60 pixels for H2O and AA for each siRNA is denoted above each pairing. (AA=α-Amanitin)

Figure 3

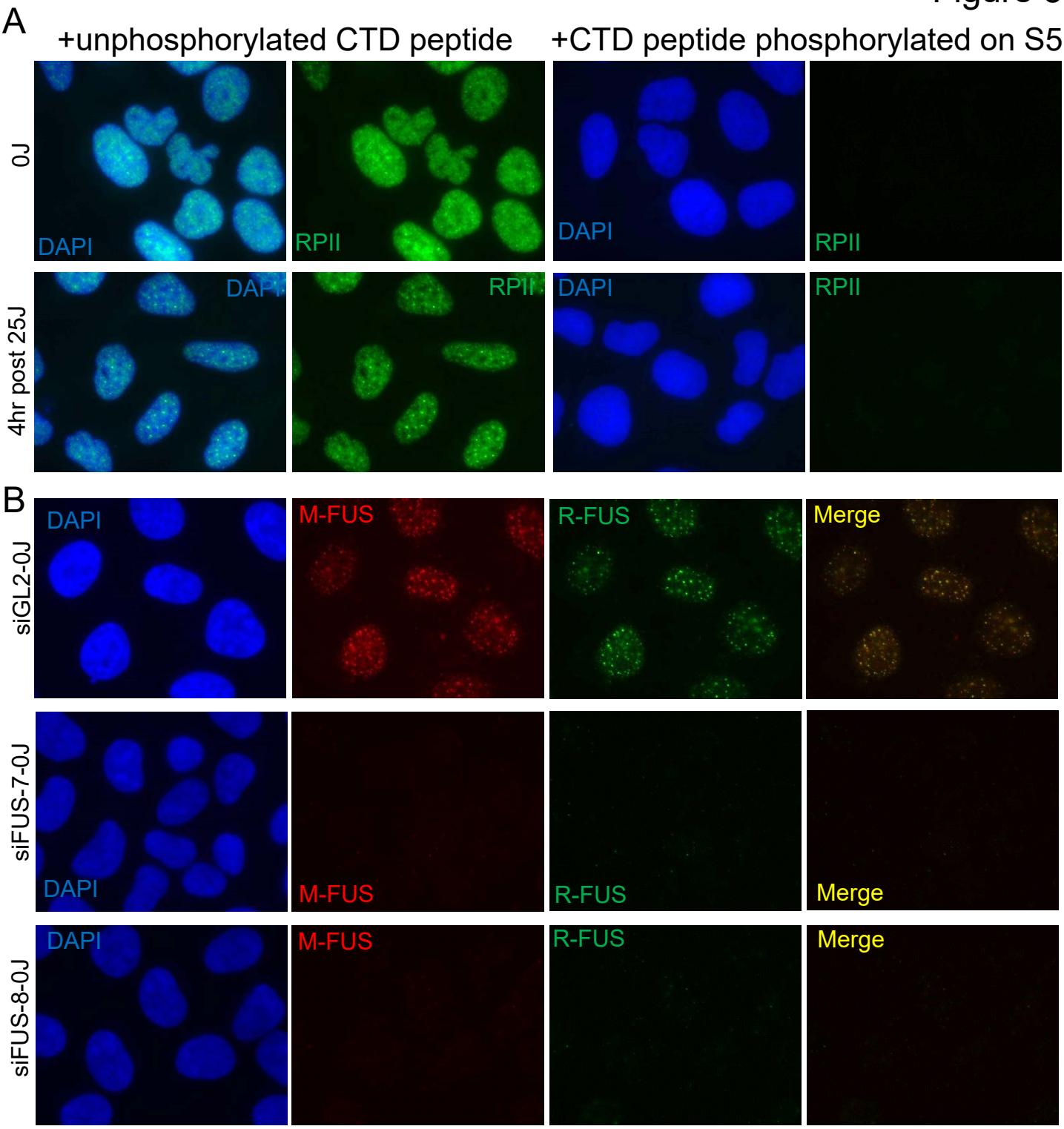
A
+unphosphorylated CTD peptide
+CTD peptide phosphorylated on S5
0J
4hr post 25J
DAPI
RPII
B
siGL2-0J
siFUS-7-0J
siFUS-8-0J
M-FUS
R-FUS
Merge

Figure 3-Specificity of the antibodies used for detection of ALS proteins at sites of post-UV transcription-associated DNA damage responses: A) An antibody that can detect the active form of RNA Polymerase II (RNA Pol II phospho-S5) was used to depict post-UV sites of transcription associated DNA damage. To assess the specificity of this antibody (labeled RPII in the photos), the antibody was incubated with two different peptides prior to being used to stain U2OS cells. In one case, the antibody was incubated with an unphosphorylated peptide encoding the C-terminal domain (CTD) of RNA Pol II (first two columns), and in the second case the antibody was incubated with a peptide encoding the CTD of RNA Pol II phosphorylated on Serine 5 (last two columns). These mixtures were used to stain U2OS cells that had been exposed to either 0J or 25J and fixed with methanol:acetic acid four hours later. Photos of DAPI-RNAPolII co-staining are shown on the left of each panel and of the RNAPolII staining alone on the right for each panel. DAPI (4',6-diamidino-2-phenylindole) is a nuclear marker. B) U2OS cells were plated on coverslips on day 1, transfected with either a control siRNA (siGL2) or one of two different FUS specific siRNAs (siFUS #7 or siFUS #8) on days 2 and 3, and fixed with methanol:acetic acid and stained for DAPI and FUS, using a mouse monoclonal FUS antibody (M-FUS) and a rabbit polyclonal FUS antibody (R-FUS), on day 4. A representative DAPI, M-FUS, and R-FUS photo is shown for siGL2, siFUS-7, or siFUS-8. *The brightness was increased by 40% in every individual photo in this figure using Microsoft PowerPoint. **These photos are best viewed on a computer screen and not on a printed paper copy.

Figure 4

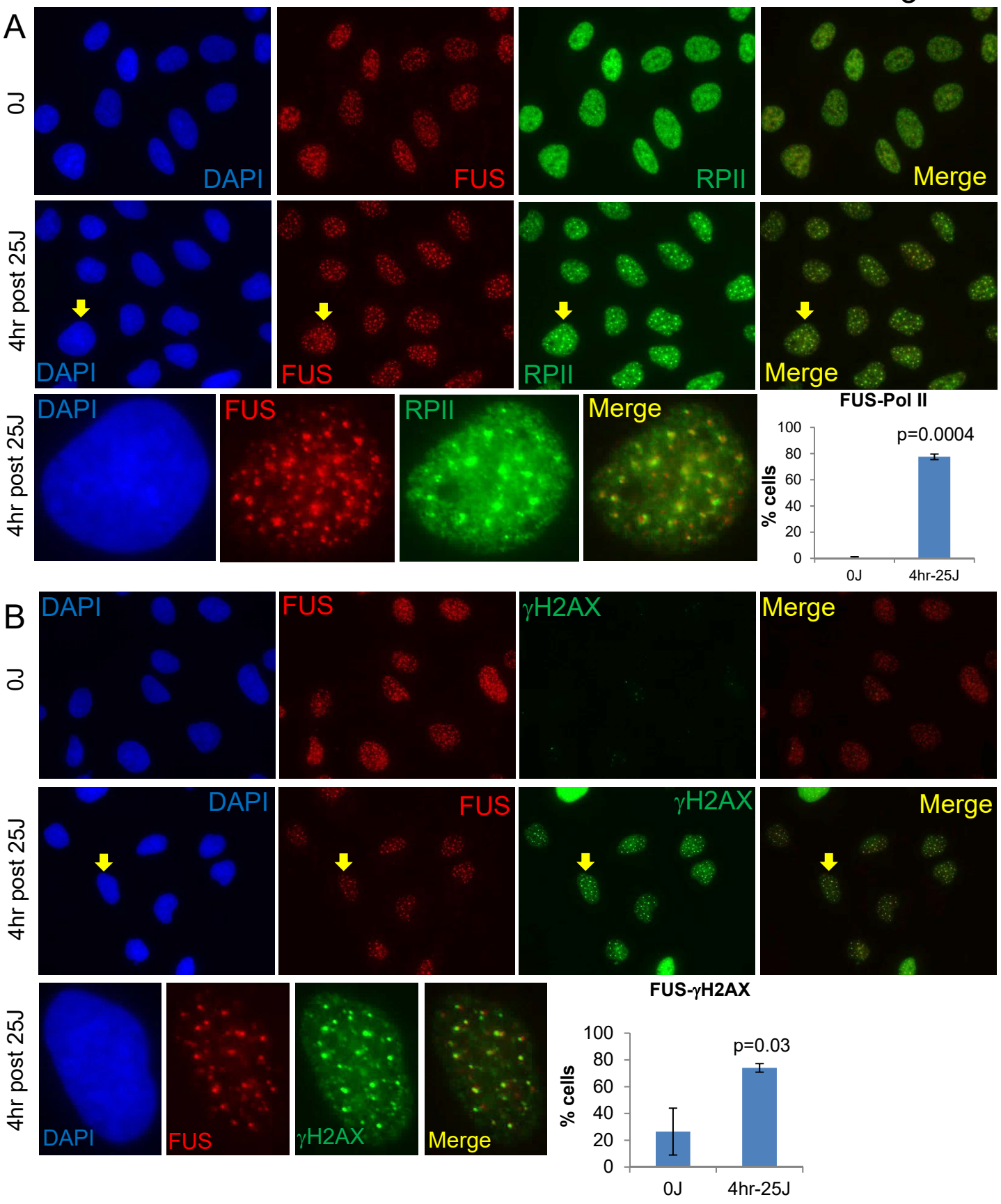
A
0J
DAPI
FUS
RPII
Merge
4hr post 25J
DAPI
FUS
RPII
Merge
4hr post 25J
DAPI
FUS
RPII
Merge
FUS-Pol II
p=0.0004
% cells
100
80
60
40
20
0
0J
4hr-25J
B
0J
DAPI
FUS
γH2AX
Merge
4hr post 25J
DAPI
FUS
γH2AX
Merge
4hr post 25J
DAPI
FUS
γH2AX
Merge
FUS-γH2AX
p=0.03
% cells
100
80
60
40
20
0
0J
4hr-25J

Figure 4-FUS localizes to sites of post-UV transcription-associated DNA damage: A and B) U2OS cells were treated with 0J or 25J, allowed to recover at 37°C for four hours, fixed with methanol:acetic acid, and co-stained for FUS and RNA Polymerase II phospho-S5 (RPII) **(A)** or FUS and γH2AX **(B).** The top row is the 0J field, the middle row is the 4 hour (hr) post 25J field, and the bottom row is a magnified cell from the 4 hour post 25J field. Yellow arrows denote a cell in the 4 hour post 25J field in which there is co-localization that has been cut out and magnified in the next row. Bar graphs representing the percentage of cells that contain greater than or equal to 3 FUS/RPII and FUS/γH2AX co-localizing foci are located next to the row of magnified single cell photos. The bars represent the average of three separate experiments, and the error bars represent the standard deviation between experiments. The p-values denoting the significance of the difference between the 0J and 4 hr post 25J results are above the 4 hr post 25J bars. *The brightness was increased by 40% in every individual photo in this figure using Microsoft PowerPoint. **These photos are best viewed on a computer screen and not on a printed paper copy.

Figure 5

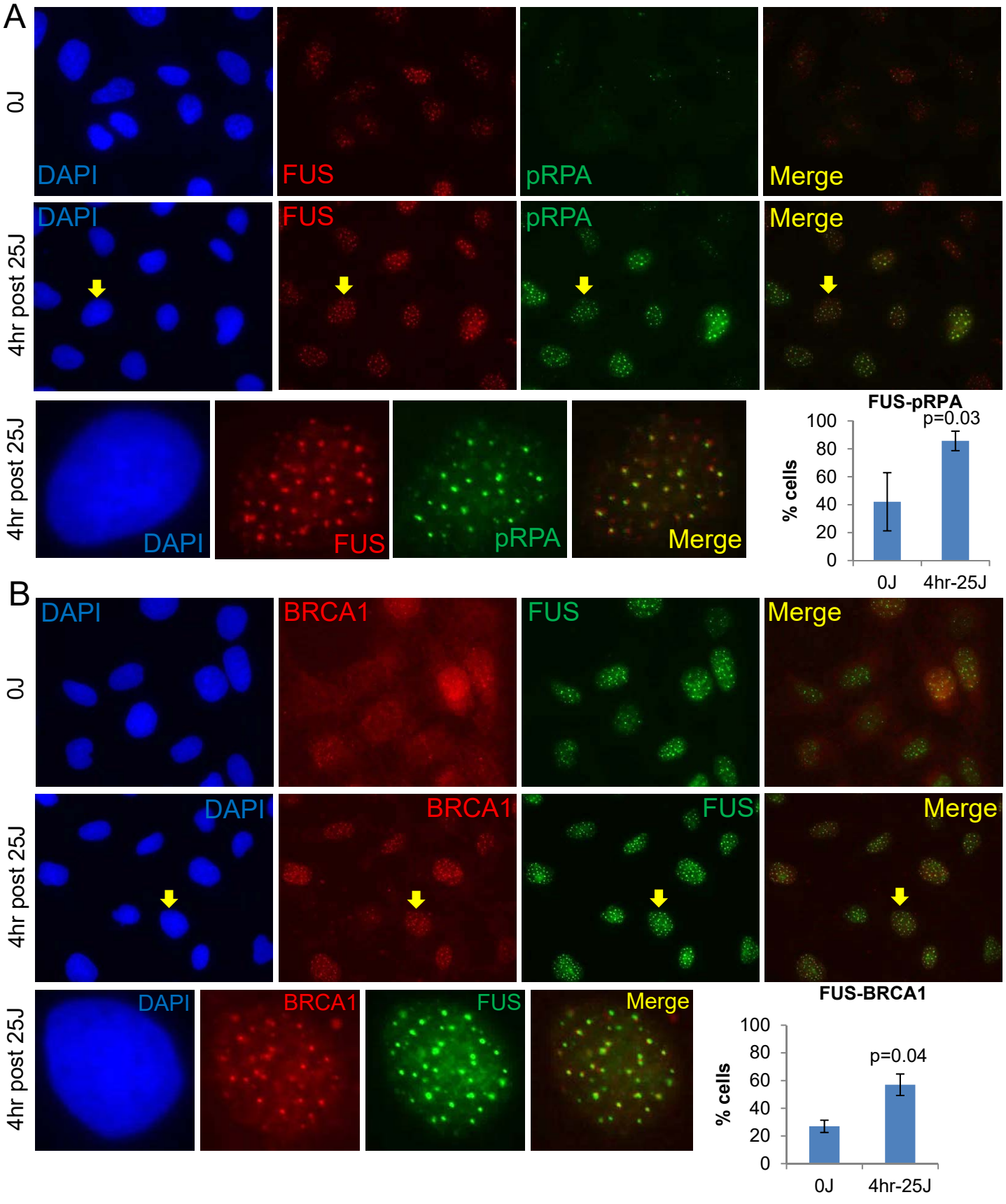
A
0J
DAPI
FUS
pRPA
Merge
4hr post 25J
DAPI
FUS
pRPA
Merge
4hr post 25J
DAPI
FUS
pRPA
Merge
FUS-pRPA
p=0.03
% cells
100
80
60
40
20
0
0J
4hr-25J
B
0J
DAPI
BRCA1
FUS
Merge
4hr post 25J
DAPI
BRCA1
FUS
Merge
4hr post 25J
DAPI
BRCA1
FUS
Merge
FUS-BRCA1
p=0.04
% cells
100
80
60
40
20
0
0J
4hr-25J

Figure 5-FUS localizes to sites of post-UV transcription-associated DNA damage with BRCA1: A and B) U2OS cells were exposed to 0J or 25J, allowed to recover at 37°C for four hours, fixed with methanol:acetic acid, and co-stained for FUS and phosphorylated (pRPA) **(A)** and FUS and BRCA1 **(B).** The top row is the 0J field; the middle row is the 4 hour (hr) post 25J field; and the bottom row is a magnified cell from the 4 hour post 25J field. Yellow arrows denote a cell in the 4 hour post 25J field in which there is co-localization. It was also isolated, magnified, and shown in its magnified state in the bottom row of A and B. Bar graphs representing the percentage of cells with greater than or equal to 3 co-localizing foci for each antibody pairing are also shown. The bars represent the average of three, separate experiments; and the error bars represent the standard deviation between experiments. The p-values denoting the significance of the difference between the 0J and 4 hr post 25J results are depicted above the 4 hr post 25J bars. *The brightness was increased by 40% in every individual photo in Microsoft PowerPoint. **These photos are best viewed on a computer screen and not on a printed paper copy.

Figure 6

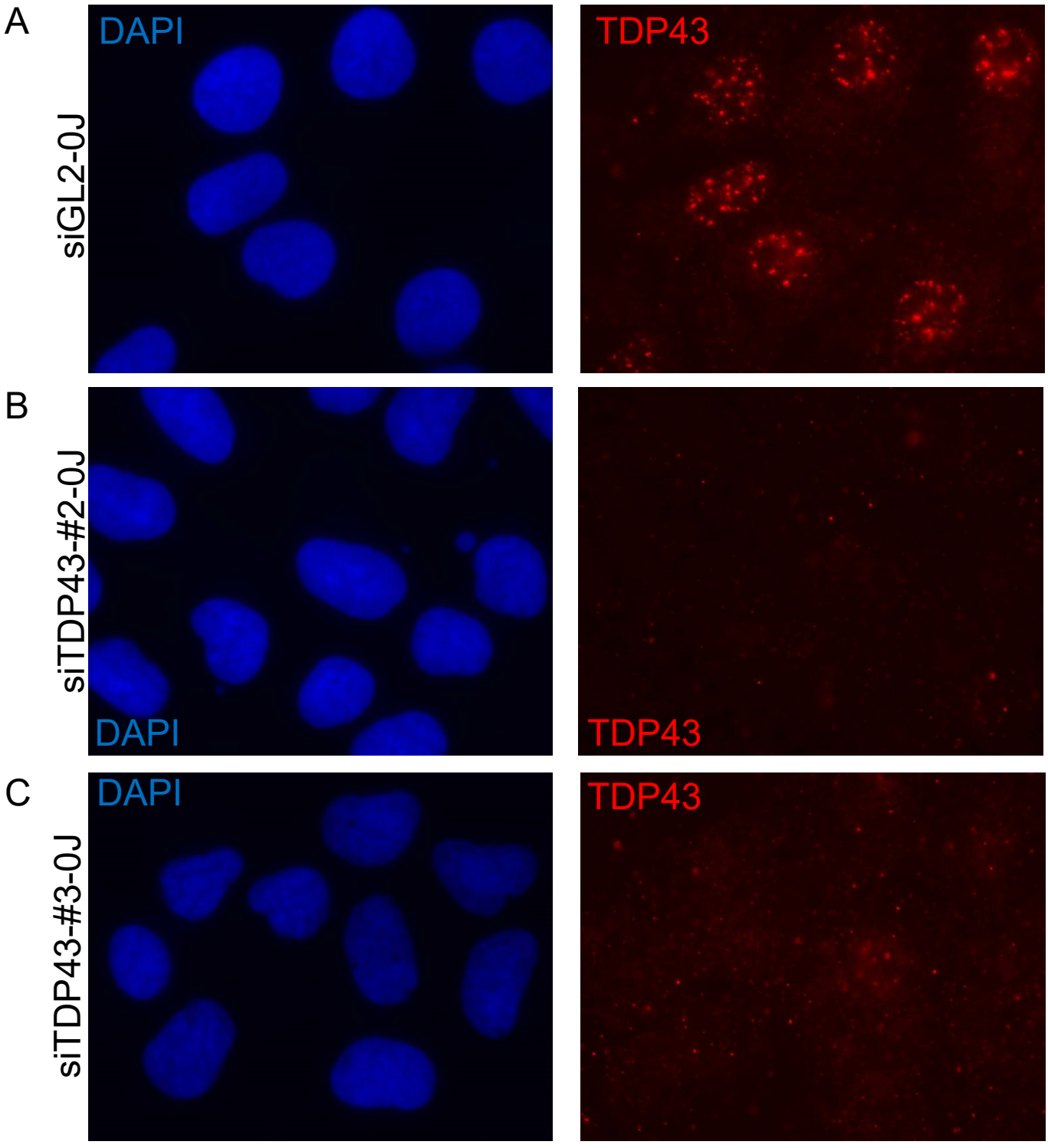
A
DAPI
TDP43
siGL2-0J
B
siTDP43-#2-0J
DAPI
TDP43
C
siTDP43-#3-0J
DAPI
TDP43

Figure 6-Antibody used for detection of TDP43: A, B, C) U2OS cells were plated on coverslips on day 1, transfected with either a control siRNA (siGL2-A) or one of two different TDP43 specific siRNAs (siTDP43 #2-B or siTDP43 #3-C), on days 2 and 3, and fixed with methanol:acetic acid and stained for DAPI and TDP43 on day 4. A representative DAPI and TDP43 photo is shown for siGL2, siTDP43-#2, or siTDP43-#3. *The brightness was increased by 40% in every individual photo in Microsoft PowerPoint. **These photos are best viewed on a computer screen and not on a printed paper copy.

Figure 7

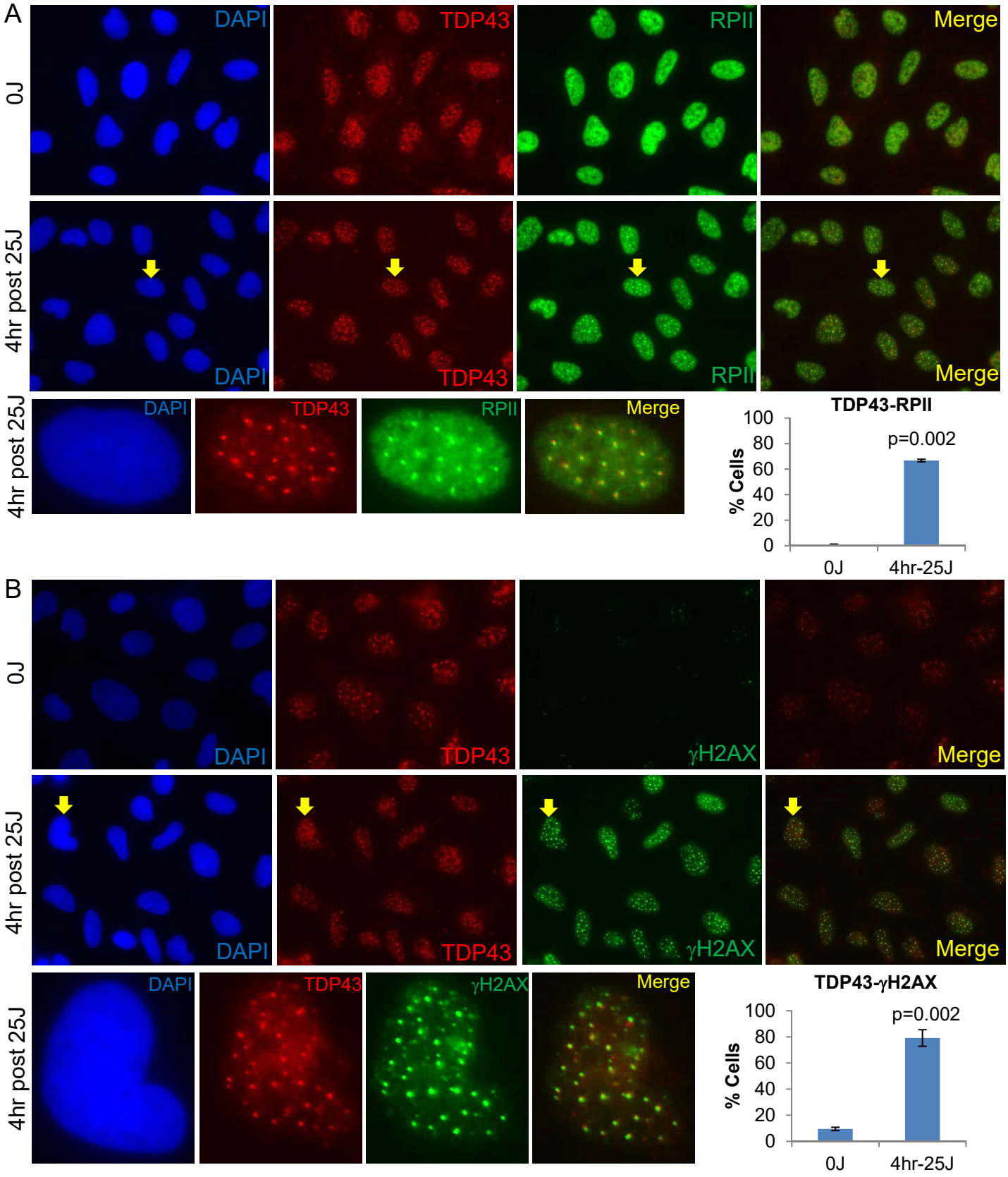
A
0J
4hr post 25J
DAPI
TDP43
RPII
Merge
TDP43-RPII
p=0.002
% Cells
100
80
60
40
20
0
0J
4hr-25J
B
γH2AX
TDP43-γH2AX

Figure 7-TDP43 localizes to sites of post-UV transcription-associated DNA damage: A and B) U2OS cells were exposed to 0J or 25J, allowed to recover at 37°C for four hours, fixed with methanol:acetic acid, and co-stained for TDP43 and RNA Polymerase II phospho-S5 (RPII) **(A)** and TDP43 and γH2AX **(B).** The top row is the 0J field; the middle row is the 4 hour (hr) post 25J field; and the bottom row is a magnified cell from the 4 hour post 25J field. Yellow arrows denote a cell in the 4 hour post 25J field in which there is co-localization that has been cut out and magnified. Bar graphs representing the percentage of cells with greater than or equal to 3 co-localizing foci for each antibody pairing are next to the row of magnified single cell photos. The bars represent the average of three, separate experiments, and the error bars represent the standard deviation between experiments. The p-values denoting the significance of the difference between the 0J and 4 hr post 25J results are depicted above the 4 hr post 25J bars. *The brightness was increased by 40% in every individual photo in Microsoft PowerPoint. **These photos are best viewed on a computer screen and not on a printed paper copy.

Figure 8

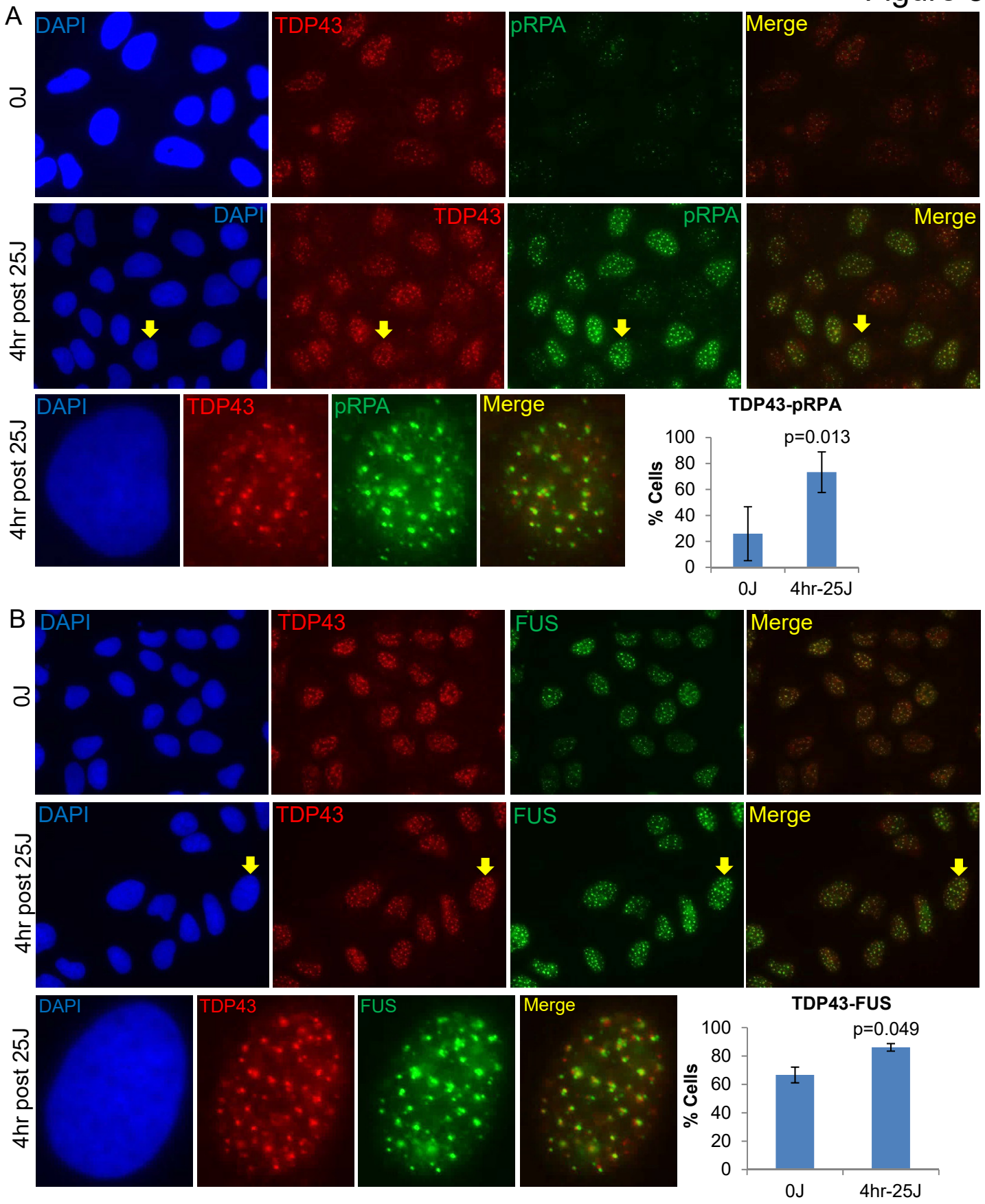
A
0J
DAPI
TDP43
pRPA
Merge
4hr post 25J
DAPI
TDP43
pRPA
Merge
4hr post 25J
DAPI
TDP43
pRPA
Merge
TDP43-pRPA
p=0.013
% Cells
100
80
60
40
20
0
0J
4hr-25J
B
0J
DAPI
TDP43
FUS
Merge
4hr post 25J
DAPI
TDP43
FUS
Merge
4hr post 25J
DAPI
TDP43
FUS
Merge
TDP43-FUS
p=0.049
% Cells
100
80
60
40
20
0
0J
4hr-25J

Figure 8-TDP43 localizes to sites of post-UV transcription associated DNA damage and co-localizes with FUS: A and B) U2OS cells were exposed to 0J or 25J, allowed to recover at 37°C for four hours, fixed with methanol:acetic acid, and co-stained for TDP43 and pRPA **(A)** or TDP43 and FUS **(B).** The top row is the 0J field; the middle row is the 4 hour (hr) post 25J field; and the bottom row is a magnified cell from the 4 hour post 25J field. Yellow arrows denote a cell in the 4 hour post 25J field in which there is co-localization that has been cut out and magnified. Bar graphs representing the percentage of cells with greater than or equal to 3 co-localizing foci for each antibody pairing are shown next to the row of magnified single cell photos. The bars represent the average of three, separate experiments; and the error bars represent the standard deviation between experiments. The p-values denoting the significance of the difference between the 0J and 4 hr post 25J results are shown above the 4 hr post 25J bars. *The brightness was increased by 40% in every individual photo in Microsoft PowerPoint. **These photos are best viewed on a computer screen and not on a printed paper copy.

Figure 9

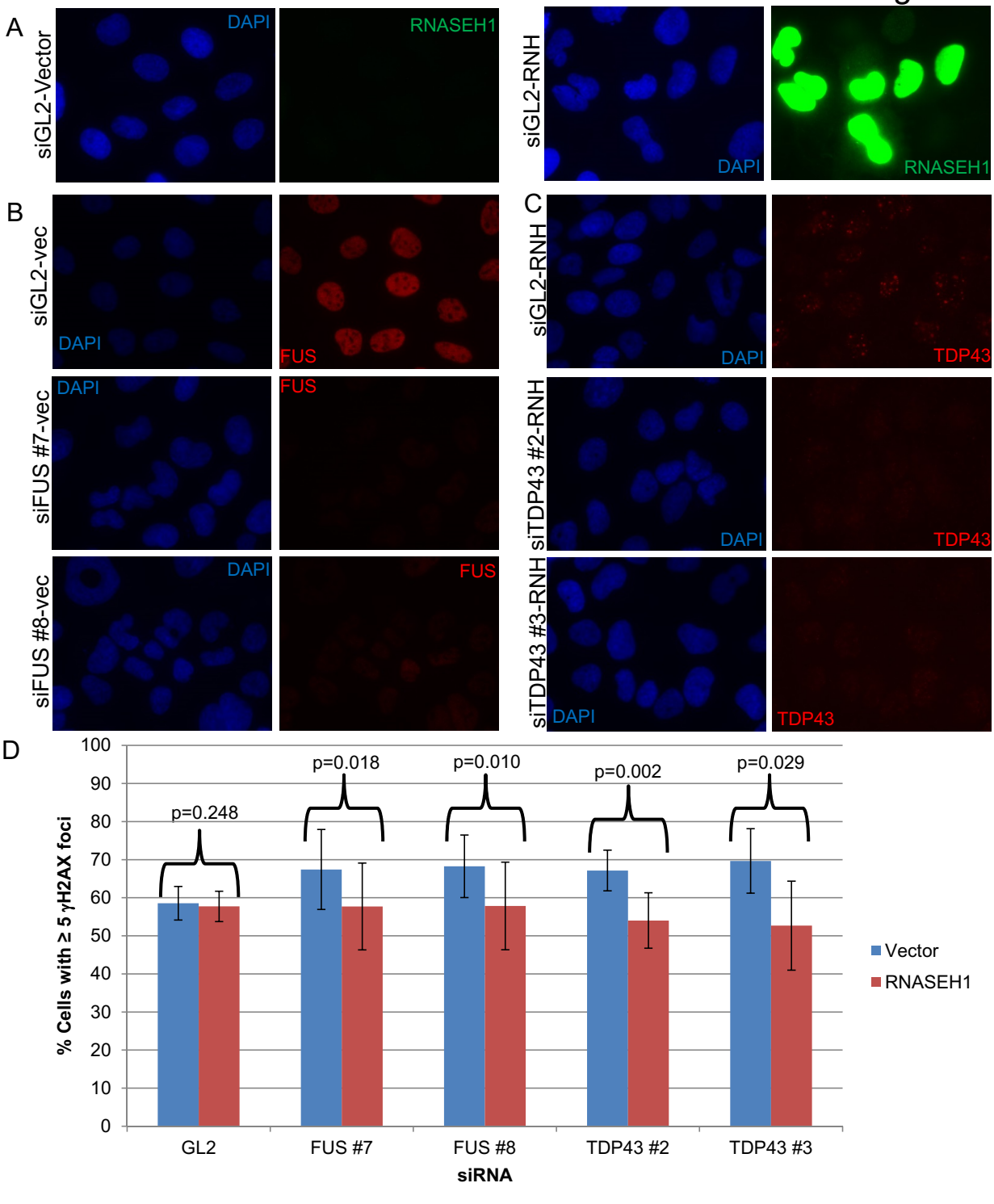
A
siGL2-Vector
DAPI
RNASEH1
siGL2-RNH
DAPI
RNASEH1
B
siGL2-vec
DAPI
FUS
siFUS #7-vec
DAPI
FUS
siFUS #8-vec
DAPI
FUS
C
siGL2-RNH
DAPI
TDP43
siTDP43 #2-RNH
DAPI
TDP43
siTDP43 #3-RNH
DAPI
TDP43
D
% Cells with ≥ 5 γH2AX foci
100
90
80
70
60
50
40
30
20
10
0
p=0.248
p=0.018
p=0.010
p=0.002
p=0.029
GL2
FUS #7
FUS #8
TDP43 #2
TDP43 #3
siRNA
Vector
RNASEH1

Figure 9-FUS and TDP43 are involved in the prevention or repair of R-loop-associated DNA damage: A) Representative images of U2OS cells co-transfected with siGL2 siRNA and either an empty vector or an RNASEH1-encoding plasmid and stained for RNASEH1. **B)** Extra coverslips from one of the four replicates of the RNASEH experiment not used for γH2AX assessment that were co-transfected with various siRNAs and empty vector (vec) were stained for FUS to assess depletion of FUS protein. Representative images are shown with DAPI on the left and FUS on the right. **C)** Extra coverslips from one of the four replicates of the RNASEH experiment not used for γH2AX assessment co-transfected with various siRNAs and RNASEH1 (RNH) were stained for TDP43 to assess depletion of TDP43 protein. Representative images are shown with DAPI on the left and TDP43 on the right. **D)** Bar graph representing the percentage of cell nuclei with greater than or equal to 5 γH2AX foci after co-transfection with various siRNAs and with either empty vector (blue bars) or RNASEH1 (red bars). Each bar represents the average of 4 separate experiments, and the error bars represent the standard deviation between those experiments. The p-values above each siRNA pair denote the significance of the difference between the vector and RNASEH1 value for each individual siRNA and were calculated using a T-test.

Figure 10

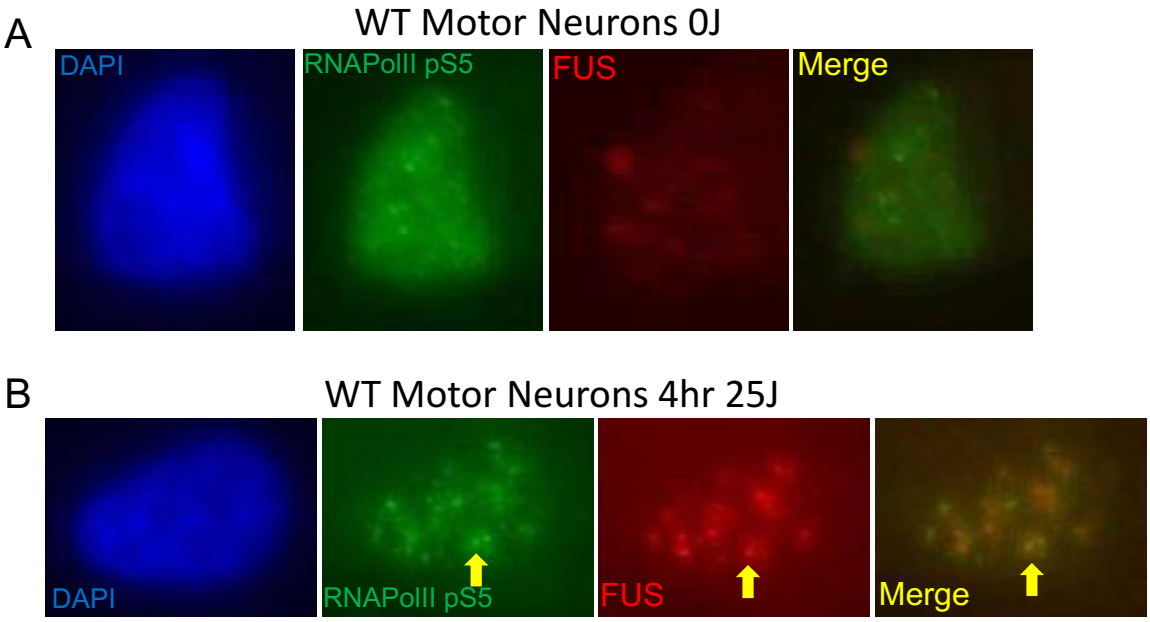
A
WT Motor Neurons 0J
DAPI
RNAPolII pS5
FUS
Merge
B
WT Motor Neurons 4hr 25J
DAPI
RNAPolII pS5
FUS
Merge

Figure 10-FUS localizes to sites of post-UV transcription-associated DNA damage in wildtype motor neurons: A and B) Motor neurons were exposed to 0J or 25J, allowed to recover at 37°C for four hours, fixed with methanol:acetic acid, and co-stained for FUS and RNA Pol II pS5. **(A)** The top row is a magnified representative photo of a motor neuron nucleus from the 0J field; **B)** the bottom row is a magnified representative photo of a motor neuron nucleus in the 4 hour (hr) post 25J field. A yellow arrow indicates a representative focus of co-localization. *The brightness was increased by 40% and the contrast decreased by 20% in every individual photo in Microsoft PowerPoint. **These photos are best viewed on a computer screen and not on a printed paper copy.